PB-243 309

SCALE CONTROL IN LIMESTONE WET SCRUBBING SYSTEMS

ARTHUR D. LITTLE, INCORPORATED

PREPARED FOR
NATIONAL ENVIRONMENTAL RESEARCH CENTER

APRIL 1975

DISTRIBUTED BY:

NTIS
National Technical Information Service
U. S. DEPARTMENT OF COMMERCE

204140

PB243309

EPA-650/2-75-031

April 1975

Environmental Protection Technology Series

SCALE CONTROL IN LIMESTONE WET SCRUBBING SYSTEMS

Reproduced by
NATIONAL TECHNICAL
INFORMATION SERVICE
US Department of Commerce
Springfield, VA. 22151

U.S. Environmental Protection Agency
Office of Research and Development
Washington DC 20460

TECHNICAL REPORT DATA
(Please read Instructions on the reverse before completing)

1. REPORT NO. EPA-650/2-75-031	2.
3.	PB 243 309
4. TITLE AND SUBTITLE: Scale Control in Limestone Wet Scrubbing Systems	5. REPORT DATE: April 1975
	6. PERFORMING ORGANIZATION CODE
7. AUTHOR(S): J. B. Berkowitz, D. Shooter, J. M. Ketteringham, L. N. Davidson, K. M. Wiig (A. D. Little Inc.); C. Y. Wen, W. J. McMichael, R. D. Nelsen Jr. (U. of W. Va.)	8. PERFORMING ORGANIZATION REPORT NO. C-75092
9. PERFORMING ORGANIZATION NAME AND ADDRESS: Arthur D. Little, Inc. Cambridge, Massachusetts 02140	10. PROGRAM ELEMENT NO. 1AB013; ROAP 21ACY-038
	11. CONTRACT/GRANT NO. 68-02-1013
12. SPONSORING AGENCY NAME AND ADDRESS: EPA, Office of Research and Development NERC-RTP, Control Systems Laboratory Research Triangle Park, NC 27711	13. TYPE OF REPORT AND PERIOD COVERED: Final; 12/72-11/73
	14. SPONSORING AGENCY CODE
15. SUPPLEMENTARY NOTES	

16. ABSTRACT: The report gives results of tests of a number of phosphate and polymeric additives--which have proven effective in controlling scale in some commercially encountered calcium-containing systems--for scale control potential in limestone wet scrubbers. Additives selected were Lime Treet; Acrysol A-1, A-3, A-5; Calnox 214 DN; Darex 40; Dequest 2000; PD-8; sodium hexametaphosphate; Calgon CL-14; sodium pyrophosphate; Versenex 80; Quadrol; and sodium tripolyphosphate. Calnox 214 DN and Calgon CL-14 were found to be particularly effective in controlling sulfate scaling in the bench scale scrubber used for testing: both reduced the rate of scaling by 75% under conditions previously shown to lead to catastrophic sulfate scaling. The kinetics of oxidation of calcium sulfite in calcium carbonate/sulfite slurries was studied and compared with the oxidation of sodium sulfite solutions. Rates of oxidation in the calcium system, found to be proportional to bisulfite ion concentration, increased in the presence of solid calcium sulfite. Therefore the rate of sulfite dissolution is a contributing factor to the oxidation under normal operating conditions. Cationic impurities, such as sodium or magnesium, which can increase bisulfite concentration in solution in the 5-6 pH range, are expected to accelerate oxidation.

17. KEY WORDS AND DOCUMENT ANALYSIS

a. DESCRIPTORS	b. IDENTIFIERS/OPEN ENDED TERMS	c. COSATI Field/Group
Air Polluation Gypsum Scrubbers Limestone Additives Scale (Corrosion) Fouling Oxidation	Air Pollution Control Stationary Sources Phosphates	13B 07A 11G 07B, 07C

18. DISTRIBUTION STATEMENT: Unlimited	19. SECURITY CLASS (*This Report*): Unclassified	21. NO. OF PAGES: 97
	20. SECURITY CLASS (*This page*): Unclassified	22. PRICE: 4.75

EPA Form 2220-1 (9-73)

PRICES SUBJECT TO CHANGE

EPA-650/2-75-031

SCALE CONTROL IN LIMESTONE WET SCRUBBING SYSTEMS

by

C. Y. Wen, W. J. McMichael, and R. D. Nelsen Jr.

University of West Virginia
Morgantown, West Virginia 26505

and

J. B. Berkowitz, D. Shooter, J. M. Ketteringham,
L. N. Davidson, and K. M. Wiig

Arthur D. Little, Inc.
Cambridge, Massachusetts 02140

Contract No. 68-02-1013
Program Element No. 1AB013
ROAP No. 21ACY-038

EPA Project Officer: R. H. Borgwardt

Control Systems Laboratory
National Environmental Research Center
Research Triangle Park, North Carolina 27711

Prepared for

U. S. ENVIRONMENTAL PROTECTION AGENCY
OFFICE OF RESEARCH AND DEVELOPMENT
WASHINGTON, D. C. 20460

April 1975

EPA REVIEW NOTICE

This report has been reviewed by the National Environmental Research Center – Research Triangle Park, Office of Research and Development, EPA, and approved for publication. Approval does not signify that the contents necessarily reflect the views and policies of the Environmental Protection Agency, nor does mention of trade names or commercial products constitute endorsement or recommendation for use.

RESEARCH REPORTING SERIES

Research reports of the Office of Research and Development, U.S. Environmental Protection Agency, have been grouped into series. These broad categories were established to facilitate further development and application of environmental technology. Elimination of traditional grouping was consciously planned to foster technology transfer and maximum interface in related fields. These series are:

1. ENVIRONMENTAL HEALTH EFFECTS RESEARCH
2. ENVIRONMENTAL PROTECTION TECHNOLOGY
3. ECOLOGICAL RESEARCH
4. ENVIRONMENTAL MONITORING
5. SOCIOECONOMIC ENVIRONMENTAL STUDIES
6. SCIENTIFIC AND TECHNICAL ASSESSMENT REPORTS
9. MISCELLANEOUS

This report has been assigned to the ENVIRONMENTAL PROTECTION TECHNOLOGY series. This series describes research performed to develop and demonstrate instrumentation, equipment and methodology to repair or prevent environmental degradation from point and non-point sources of pollution. This work provides the new or improved technology required for the control and treatment of pollution sources to meet environmental quality standards.

This document is available to the public for sale through the National Technical Information Service, Springfield, Virginia 22161.

Publication No. EPA-650/2-75-031

TABLE OF CONTENTS

		Page
I.	CONCLUSIONS	1
	A. Control of Scaling	1
	B. Sulfite Oxidation	2
	C. Mathematical Modeling	3
II.	RECOMMENDATIONS	4
	A. Control of Calcium Sulfite Scale	4
	B. Control of Calcium Sulfate Scale	4
	C. Modeling of Scrubber Systems	5
III.	BACKGROUND	6
IV.	METHODS OF SCALE CONTROL	8
	A. Model of Scale Formation	
	B. Experimental Results	21
	1. pH Control	21
	2. Seed Crystals	23
	3. Additives	27
	C. Implications of the Scaling Model for Scrubber Operation	36
V.	SULFITE OXIDATION	37
	A. Introduction	37
	B. Evaluation of Literature Data on Sodium Sulfite	40
	C. Experiments with Sodium Sulfite	43
	D. Experiments with Calcium Sulfite	52

TABLE OF CONTENTS

(continued)

		Page
VI.	MATHEMATICAL MODEL OF PACKED BED SCRUBBER	58
	A. Material Balances	58
	B. Absorption Parameters	69
	C. Scrubber Simulation	79

LIST OF FIGURES

IV-1.	Typical Pressure Drop along the Length of the Packed Bed Versus Operating Time - Run 39.	9
IV-2.	Generalized Pressure Drop Correlation	11
IV-3.	Comparison of the Measured Pressure Drop across the Packed Bed with the Pressure Drop Predicted by Standard Correlations Assuming the Intrinsic Rate of Scaling Constant - Run 39.	14
IV-4.	Comparison of the Measured Pressure Drop across the Packed Bed with the Pressure Drop Predicted by Standard Correlations Assuming the Intrinsic Rate of Scaling Constant - Run 40.	15
IV-5.	Comparison of the Measured Pressure Drop across the Packed Bed with the Pressure Drop Predicted by Standard Correlations Assuming the Intrinsic Rate of Scaling Constant - Run 41.	16
IV-6.	The Functional Relationship between α, a Constant Appearing in the Pressure Drop Correlation for Packed Beds Given by Equation (IV-5) and the Void Fraction of the Packed Bed, ε.	18
IV-7.	The Functional Relationship between β, a Constant Appearing in the Pressure Drop Correlation for Packed Beds Given by Equation (IV-5) and the Void Fraction of the Packed Bed, ε.	19
IV-8.	Scale Analysis versus Scale Weight.	31

LIST OF FIGURES (continued)

		Page
V-1.	Oxidation Rate vs. Impeller Rotation (A Representative Curve for a Stirred Vessel).	39
V-2.	Log Oxidation Rate vs. Log Partial Pressure of Oxygen for 400 mmoles/l Na_2SO_3 Feed (Impeller Rotation = 375 RPM).	47
V-3.	Log Oxidation Rate vs. Log $[1/H^+]$ for Na_2SO_3 Feed at 4% Oxygen (Impeller Speed = 600 RPM), Tables 1 and 3.	49
V-4.	Log Rate/$[\frac{1}{H^+}]^{0.12}$ vs. Log Impeller Rotation for Na_2SO_3 Feed at 4% Oxygen, Tables 7, 8 and 9.	50
V-5.	Log Oxidation Rate vs. Log CSTR Sulfite Concentration for $CaSO_3$ Supernatant Feed (4% Oxygen, Impeller Speed = 625 RPM)	54
VI-1.	Recycle Scrubber System.	59
VI-2.	Equilibrium Concentration of Total Sulfur, Carbon and Calcium and the Delta Concentration as a Function of pH. Solution Saturated with $CaSO_3$, Temperature is 125°F and Partial Pressure of CO_2 Restricted to Less Than 0.2 atm.	63
VI-3.	Titration Diagram for the $CaCO_3$-SO_2 System.	66
VI-4.	The "Average" Enhancement Factor for Mass Transfer in the Liquid Film in Packed Bed as a Function of the pH of the Holding Tank in Scrubber Recycle System.	77
VI-5.	Comparison of the Percent SO_2 Removal from the Flue Gas with the Predicted Percent SO_2 Removal Calculated Using the Observed pH of the Holding Tank to Evaluate the Enhancement Factor.	80
VI-6.	Graphical Determination of the Operating Point of the Scrubber-Recycle System.	82
VI-7.	Comparison of the Calculated and the Measured Holding Tank pH for the A. D. Little Scrubber-Recycle System.	84
VI-8..	Comparison of the Calculated and Experimentally Observed Percent SO_2 Removal in Experimental Scrubber-Recycle System.	85
VI-9.	Graphical Determination of the Operating Point of the Scrubber-Recycle System with a Comparison of the Effects of Either Having No Sulfate or Sulfate Saturated Slurries.	87

LIST OF TABLES

		Page
IV-I.	Pressure Drop as a Function of Time Predicted from Figure IV-2 for Run 39.	13
IV-2.	Pressure Drop as a Function of Time on Line Predicted by Equation (IV-6) for Run 39.	17
IV-3.	Summary of Calcium Sulfite Scaling Data	22
IV-4.	Summary of Calcium Sulfate Seeding Data	26
IV-5.	Anti-Scaling Additives Selected for Preliminary Screening	30
IV-6.	Comparison of Anti-Scaling Additives in Screening and Bench-Scale Scrubber Tests.	34
IV-7.	Summary of Additive Data	35
V-1.	Summary of Literature Data on Reaction Order	42
V-2.	Comparison of Calculated and Measured Oxidation Rates	45
V-3.	Effect of Gas Flow Rate on Oxidation Rate	45
V-4.	Summary of Oxidation Rates for Calcium	53
VI-I.	Gas Side Mass Transfer Coefficients for Physical Absorption for A. D. Little's Packed Column	71
VI-2.	Range of Data Used in the Construction of Figure VI-4.	78
VI-3.	Simulation of Run 14	88

I. CONCLUSIONS

A. Control of Scaling

1. Calcium sulfite scale can be minimized by limiting the addition of calcium carbonate (stoichiometry) to control the pH at the inlet to the scrubber to below pH 6.0. (For the bench scale scrubber the range 5.6 - 6.0 is appropriate). Under these conditions the rate of scale formation is only about 15% of that at higher pH (>6.2).
2. Operation at reduced pH causes a reduction in sulfur dioxide removal efficiency of 15-20% in the bench scale scrubber. In full scale units, this can be recovered by altering scrubber design to increase scrubber absorption efficiency.
3. The rate of calcium sulfite scaling is three times higher at 125°F than at 100°F. This illustrates the importance of operating at the lowest practicable temperature.
4. Rapid calcium sulfate scaling occurs due to oxidation when the carbonate slurry feed is saturated with calcium sulfate in the absence of solid sulfate even at low pH (when sulfite scaling is controlled.)
5. The presence of 1% gypsum seed crystals decreases the rate of scaling to about 40% of that observed in saturated sulfate solutions containing no sulfate solid. In our experiments, concentrations of gypsum greater than 1% did not appear to further reduce the scaling rate, contrary to published observations that 3-5% gypsum seed crystals are optimum.

6. Calcium sulfate hemi-hydrate and anhydrite crystals are ineffective as seeding agents, and in fact accelerate the rate of calcium sulfate scale formation.

7. Out of six anti-scaling additives tested, two were found to be particularly effective in controlling sulfate scaling in the bench scale scrubber. These are Calnox 214 DN and Calgon CL-14, which reduced the rate of scaling at 125°F by 75%, compared to an unseeded carbonate slurry saturated with calcium sulfate. As an additional benefit these additives allow pH control below pH 6 at a higher stoichiometry which improves the SO_2 removal efficiency by 15-20%.

8. The combined use of the Calnox 214 DN additive and gypsum seed crystals has a synergistic effect, reducing the rate of scaling below that of either seed crystals or additives alone.

B. Sulfite Oxidation

1. Oxidation of sodium sulfite solutions (used as a model) was controlled by liquid phase mass transport in the range of experimental conditions studied. Oxygen concentration was the most important variable; the oxidation rate was independent of total sulfite concentration in solution, but inversely proportional to hydrogen ion concentration (pH 9 - pH 3).

2. Oxidation of calcium sulfite (in calcium carbonate/calcium sulfate slurries) was independent of pH because the rate of solid dissolution is sufficiently rapid to offset the low equilibrium solubility of calcium sulfite above pH 6. Addition of copper sulfate as a potential catalyst and Calnox 214 DN as a potential inhibitor did not affect the oxidation rates.

3. Sulfite in calcium sulfite/calcium carbonate slurries oxidizes somewhat more rapidly than calcium sulfite slurries at pH 4 and about equally rapidly at pH 7. [Above pH 6, oxidation caused an increase in solution pH; below pH 6, oxidation caused a decrease in pH. This is in contrast to results with saturated calcium sulfite solutions where a decrease in pH was always observed.]

C. Mathematical Modeling

1. Pressure drop curves across the scrubber as a function of time obtained during scrubber operation can be characterized in terms of scale formation (i.e., a constant intrinsic rate of scale formation). This correlation can be used to estimate the operating time on line before the scrubber will become inoperable due to flooding.

2. The bench scale scrubber-recycle system can be simulated quite accurately with a simple procedure consisting of three steps: 1) constructing a titration graph from equilibrium information which describes the equilibrium characteristics of the makeup slurry as sulfur dioxide is added to it, 2) determining the sulfur dioxide absorption characteristics of the scrubber, and 3) finding the conditions under which the equilibrium characteristics of the makeup slurry and the scrubber characteristics are satisfied simultaneously (i.e., finding the operating point). The general form of this model should be applicable to other scrubber systems.

II. RECOMMENDATIONS

A. Control of Calcium Sulfite Scale

Calcium sulfite scaling should be minimized by controlling scrubber pH. In the bench scale scrubber with calcium carbonate slurries, inlet pH is about 6.0, in the larger EPA pilot plant scrubber* the optimum appears to be about pH 6.2. Conditions in a full scale scrubber will obviously differ somewhat, but the pH should not exceed 6.0 at points in the scrubber where significant amounts of calcium sulfite are being formed. pH control does cause some reduction in sulfur dioxide absorption efficiency; to minimize the loss, the scrubber exit pH should be greater than pH 5.6. The scrubber liquor should be circulated at the lowest practicable temperature; 100°F is considerably better than 125°F in terms of scale control. Operation at the lower temperatures also has the advantage of improving absorption efficiency.

B. Control of Calcium Sulfate Scale

There are two opposite operating modes which can be used to minimize calcium sulfate scale. The first alternative is to minimize oxidation in the system and operate unsaturated with respect to calcium sulfate in solution. This can be achieved by sealing the hold tank to reduce oxidation below 20%, calcium sulfate is then precipitated from the system as a mixed crystal with calcium sulfite.

---

*R. Borgwardt, E.P.A. Progress Report 8 March 1973.

The second alternative is to maximize oxidation by sparging air into the hold tank to give oxidation rates in excess of 50%. Calcium sulfate scaling from the saturated solution is then controlled by the presence of gypsum seed crystals. When operating in this mode it is also essential to maintain a concentration of at least 1% gypsum seed crystals throughout the scrubber loop. The use of an additive, such as Calnox 214 DN in addition to the gypsum seed crystals, has a synergistic effect, reducing the rate of scaling even further.

C. Modeling of Scrubber Systems

Using the data from the bench scale scrubber, it has been shown that the absorption efficiency and the rate of scaling can be estimated. Further work should be carried out to extend these models to larger scrubbers such as the EPA pilot plant, the Shawnee demonstration plant and full scale systems.

III. BACKGROUND

Scaling in limestone wet scrubbers is a complex phenomenon resulting from two main reactions. These are the precipitation of calcium sulfite and the precipitation of calcium sulfate (gypsum). In some cases the unstable intermediate calcium sulfate hemi-hydrate may also be formed.

Since the objective of the limestone wet scrubbing process is to remove sulfur dioxide from the gas phase as calcium sulfite solid, precipitation of solid phase cannot be eliminated overall. Efforts to control calcium sulfite scale, in particular, must be aimed therefore at preventing or minimizing precipitation in the scrubber column while encouraging complete precipitation of calcium sulfite at a more appropriate location such as the hold tank.

Previous work* has shown a number of ways one can minimize sulfite scaling in the scrubbing column. For example, a high liquid-to-gas ratio (L/G) gives improved mechanical washing of the column, reduces the make of calcium sulfite per pass, and gives a lower liquid residence time in the column, therefore inducing more precipitation in the hold tank. Reduction of the liquid temperature also slows the rate of calcium sulfite precipitation and again provides less scaling in the scrubber column.

Scaling by calcium sulfate must be treated differently. It is not possible to eliminate oxygen from the system entirely because of the 4% oxygen present in the flue gas. Various inhibitors have been suggested for controlling oxidation, but none have so far been adequately demonstrated. In parallel with

*Evaluation of Problems Related to Scaling in Limestone Wet Scrubbing. EPA R2-73-214, April 1973.

our work, R. Borgwardt* has shown in the EPA pilot plant scrubber that most of the sulfite oxidation occurs in the hold tank and therefore oxidation can be minimized by sealing the hold tank from access to air. When this is carried out, the calcium sulfate is removed as a mixed crystal with the calcium sulfite and consequently the solution is always unsaturated with respect to calcium sulfate. If the oxidation level is higher than 20%, then sulfate is precipitated directly and can cause scaling problems.

An alternative mode of operation is to maximize oxidation in the scrubber loop, for example by encouraging oxidation in the hold tank through sparging with oxygen during precipitation of the calcium sulfite. This improves the settling rate of solids from the process but introduces the danger of rapid sulfate scaling from supersaturated solutions in the scrubbing column. Early work by Lessing** has shown that supersaturation can be controlled by the addition of calcium sulfate seed crystals which can act as nucleation sites in preference to the scrubber surfaces. Other work, primarily in desalination, has indicated that scaling can be controlled by various types of threshold additives which may function by reducing the extent of supersaturation, or by surface activity which prevents deposition of calcium sulfate on the scrubber surfaces. Both seeding and the use of threshold additives have been investigated in this report together with a study of the factors affecting oxidation.

---

*R. Borgwardt, EPA Progress Report #3, October 1972.

**Lessing, R. J. Soc. Chem. Ind. Transactions & Communications, November 1938, pp. 373-388.

IV. METHODS OF SCALE CONTROL

This chapter presents the development of a mathematical treatment of scale formation. This treatment is used to evaluate data from experiments to control calcium sulfite scaling by modification of operating conditions and ways to control calcium sulfate scaling by the use of seed crystals and anti-scaling additives.

A. Model of Scale Formation

In this section, we show that pressure drop-time curves can be predicted reasonably well by assuming that the rate of scale formation is a constant over the period from initial pressure drop increase to the point of "catastrophic" scaling. This calculated rate of scaling can serve as a quantitative indicator for judging scale inhibitors and also,with further analysis,provides information on the kinetics of scale formation.

Pressure Drop in Packed Beds

In the analysis to follow, it will be assumed that the pressure drop increase in a packed bed is due to scale formation on the packing pieces only and that the pressure drop across the distributor, etc., is constant throughout the scaling process. This assumption is consistent with our observation that the majority of the scale formation is on the packing pieces.

A typical pressure drop-time curve is shown in Figure IV-1. The initial pressure drop is due primarily to the pressure drop across the distributor, etc. As the scaling process proceeds, the pressure drop across the packing increases almost linearly and after about 24 hours as shown in Figure IV-1 for Run 39, the pressure drop increases exponentially. At about 32 hours (in this particular

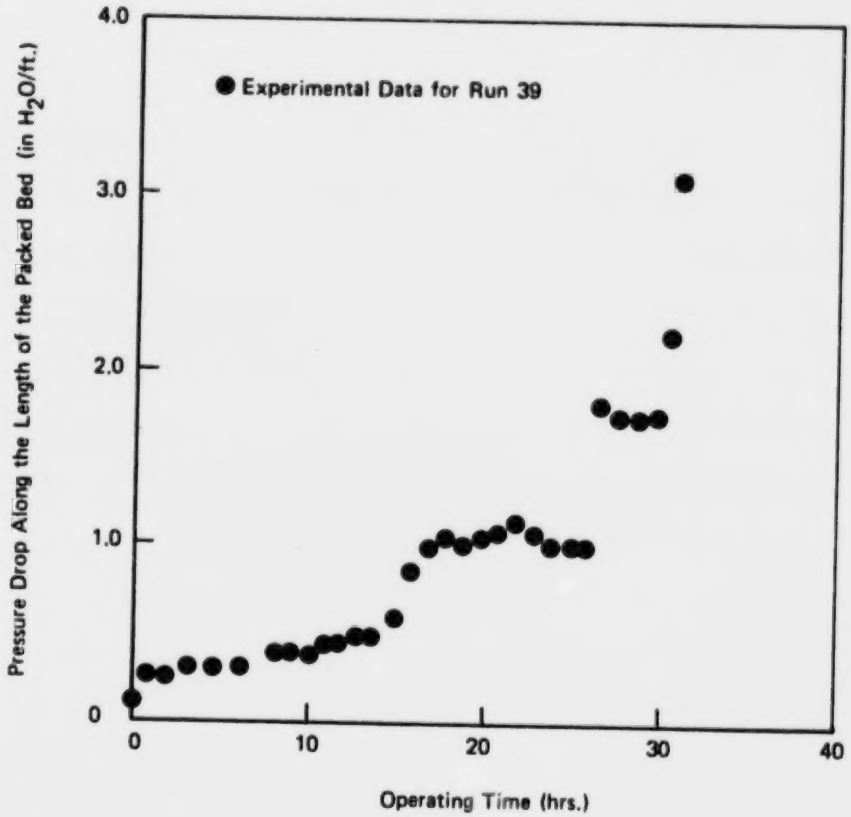

FIGURE IV–1 TYPICAL PRESSURE DROP ALONG THE LENGTH OF THE PACKED BED VERSUS OPERATING TIME – RUN 39

case) the rate of pressure drop increase is extremely large. This is the point of "catastrophy". It can also be seen that at this point the pressure drop per unit length of packing is about 3 in. H_2O/ft which corresponds to flooding in a randomly packed column regardless of the type of packing.

A generalized correlation for pressure drop and flooding has been reported by Leva[4] and is shown in Figure IV-2. From this figure it can be seen that once the process conditions are fixed, the pressure drop and flooding point are only a function of the specific packing surface, a, and the fractional voids, ε, and that the pressure drop increases with decreasing fractional voids.

It is envisioned that in the scaling process the pressure drop is due to change in the specific surface and/or the fractional voids as a result of scale formation on the packing pieces. Characterization of the change in the specific surface as a function of the amount of scale deposited is difficult. The packing pieces can be thought of as equivalent spheres with scale formation increasing the effective diameter of these spheres; hence, increasing the surface area per unit volume of column. However, because the packing pieces are in contact with each other, the scale formation could fill in small crevices between the packing pieces causing a decrease in the surface area of the packing. Thus, whether there is an increase or decrease in the specific area with increase in the amount of scale cannot be answered at this time. For the present the specific area will be assumed constant.

The fractional voids can be determined by a simple mass balance over the column:

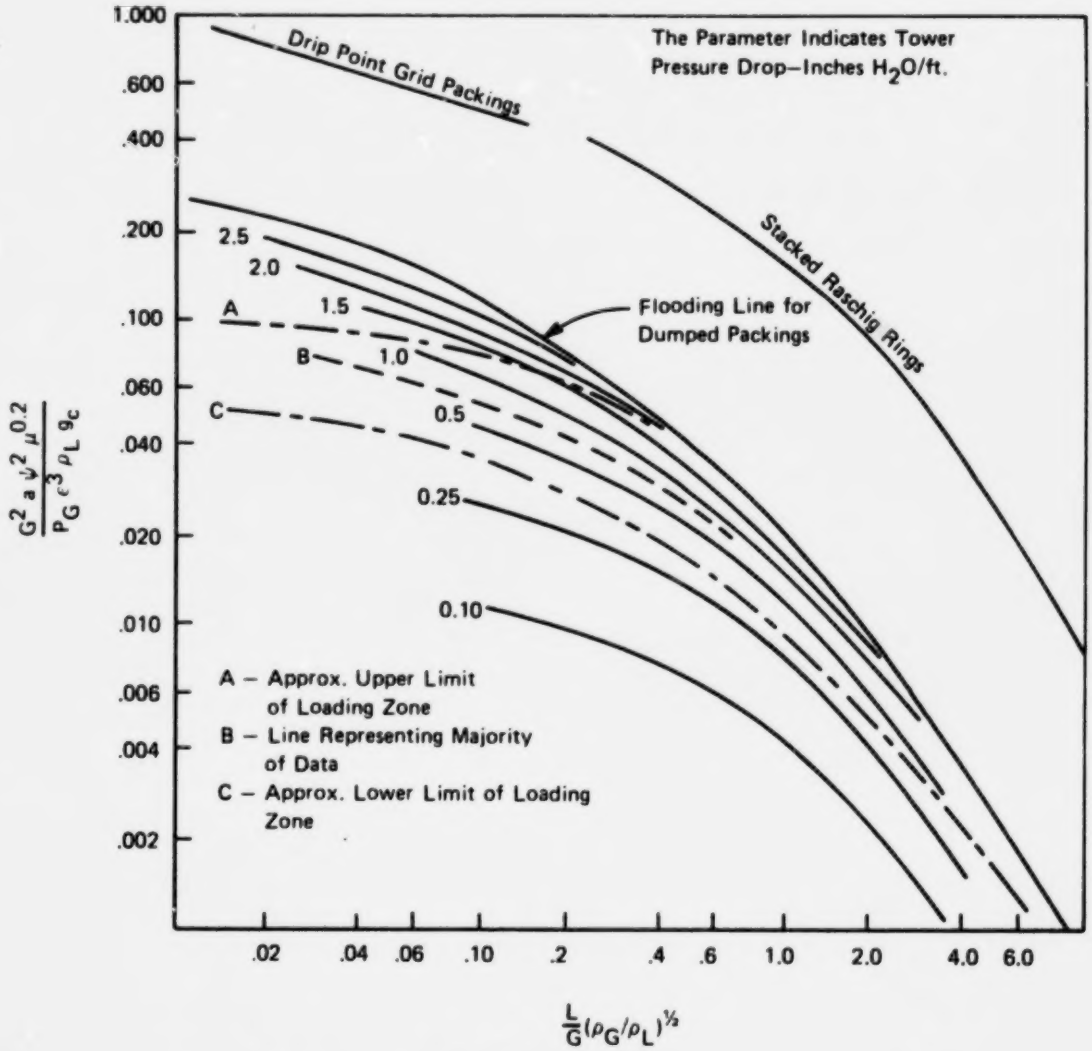

L = liquid mass velocity, lb./(hr.) (sq. ft.)
G = gas mass velocity, lb./(hr.) (sq. ft.)
ρ_L = liquid density, lb./cu. ft.
ρ_G = gas density, lb./cu. ft.
a = specific packing surface, sq. ft./cu. ft.
g_c = gravitational conversion factor, 4.173×10^8 (lb. mass) (ft.)/(lb. force) ($hr.^2$)
ϵ = fractional voids (dimensionless)
μ = viscosity of liquid, centipoise
ψ = ratio density of water to density of new liquid (dimensionless)

FIGURE IV–2 GENERALIZED PRESSURE DROP CORRELATION

rate of change in the solid volume = volumetric rate of scale formation

$$\frac{dV}{dt} = V_e r \qquad \text{(IV-1)}$$

Where V is the volume of the solids, (cm^3),

V_e is the empty volume of the column, (cm^3), and

r is the intrinsic rate of scale formation, (hr^{-1}).

Noting that $V = V_e (1-\varepsilon)$ (where ε is the void fraction) and substituting this into Equation IV-1 gives

$$-\frac{d\varepsilon}{dt} = r \quad \text{with } \varepsilon = \varepsilon_o \text{ at } t = t_o \qquad \text{(IV-2)}$$

Assuming that the intrinsic rate, r, is constant, Equation IV-2 can be integrated to give

$$\varepsilon - \varepsilon_o = -r(t-t_o) \qquad \text{(IV-3)}$$

Where the subscript "o" refers to the point at which the initial increase in pressure drop is observed.

The intrinsic rate of scale formation can be evaluated from the following data for Run 39 (see Figure IV-1).

$t_o = 0$ $\varepsilon_o = 0.78$ for 1/2" Intalox Saddles

The time, t, can be chosen as the time at which flooding occurs or t = 32 hours. The fractional voids at flooding can be evaluated using Figure IV-2. For Run 39, ε is found to equal 0.46. Using Equation IV-3

$$r = \frac{0.78 - 0.46}{32} = 0.010 \text{ hr}^{-1} \qquad \text{(IV-4)}$$

Again using Figure IV-2, values of the pressure drop per unit length can be assumed and corresponding values of the void fraction, ϵ, calculated. The result of these manipulations are shown in Table IV-I.

TABLE IV-I

Pressure Drop as a Function of Time Predicted from Figure IV-2 for Run 39

$\frac{\Delta P}{Z}$ column	$\frac{\Delta P}{Z}$ Total, $\frac{\text{in } H_2O}{\text{ft}}$	ϵ	t(hr)
0.25	0.48	0.718	10
0.50	0.73	0.604	18
1.00	1.23	0.538	25
1.50	1.73	0.504	28
2.00	2.23	0.484	30
2.50	2.73	0.471	31
3.00	2.23	0.461	32

Since the intrinsic rate of scale formation, r, can be evaluated as described above; void fraction as a function of time is given by Equation (IV-3). Numerical results are shown by columns (3) and (4) of Table IV-1. Thus Table IV-1 shows the relationship between the pressure drop and time which is plotted as a dashed line and compared with experimental data in Figure IV-3. Similar comparisons for Runs 40 and 41 are shown in Figures IV-4 and IV-5, respectively. It can be seen from Figures IV-3, 4 and 5 that at pressure drops per unit length of column greater than about 0.5 in. H_2O/ft the agreement between the pressure drop predicted by the general correlation given in Figure IV-2 and experimental data is very good.

Below a pressure drop per unit length of column of 0.5 in. H_2O/ft. another pressure drop correlation given by Leva[4] can be used to predict pressure drop versus time. The correlation is:

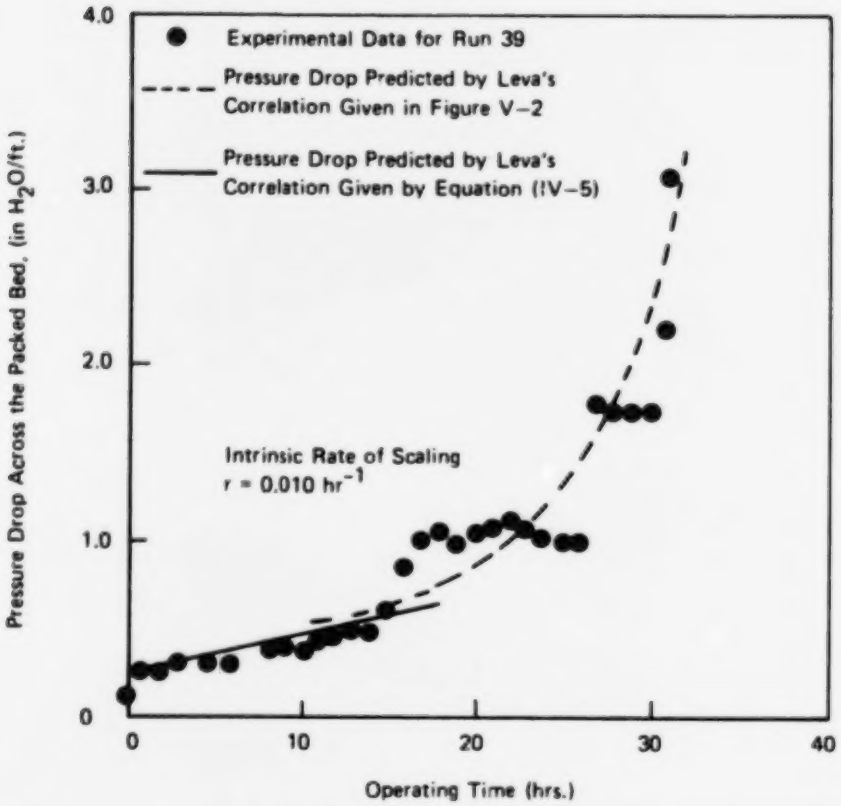

FIGURE IV–3 COMPARISON OF THE MEASURED PRESSURE DROP ACROSS THE PACKED BED WITH THE PRESSURE DROP PREDICTED BY STANDARD CORRELATIONS ASSUMING THE INTRINSIC RATE OF SCALING CONSTANT

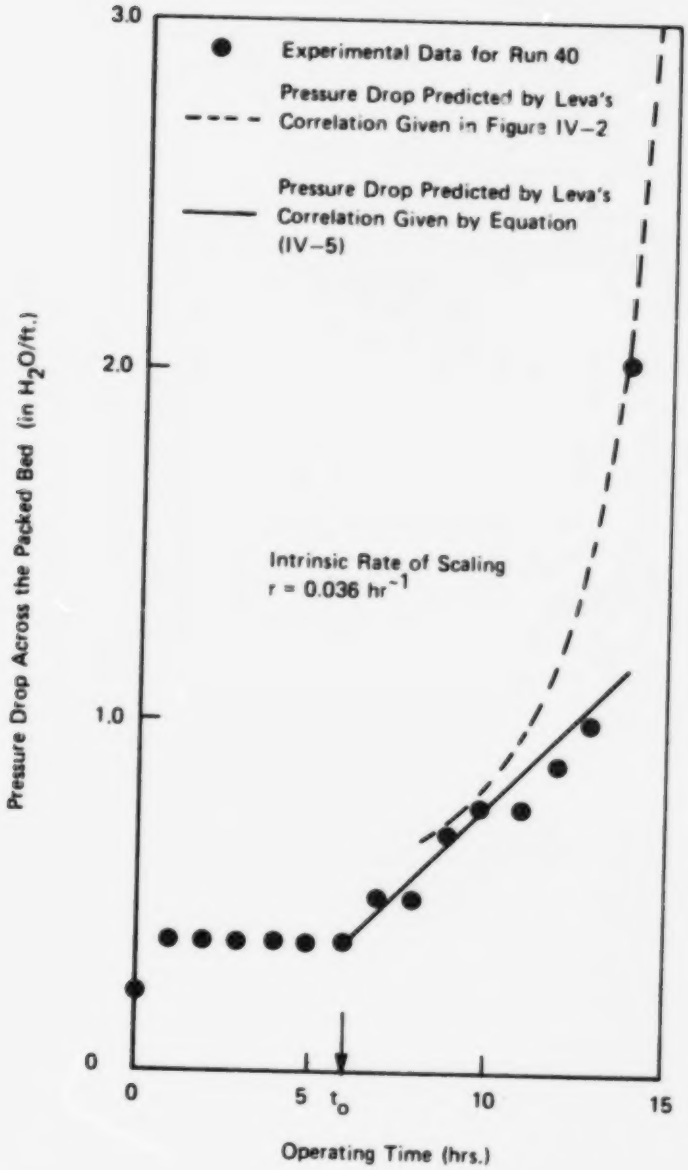

FIGURE IV–4 COMPARISON OF THE MEASURED PRESSURE DROP ACROSS THE PACKED BED WITH THE PRESSURE DROP PREDICTED BY STANDARD CORRELATIONS ASSUMING THE INTRINSIC RATE OF SCALING CONSTANT

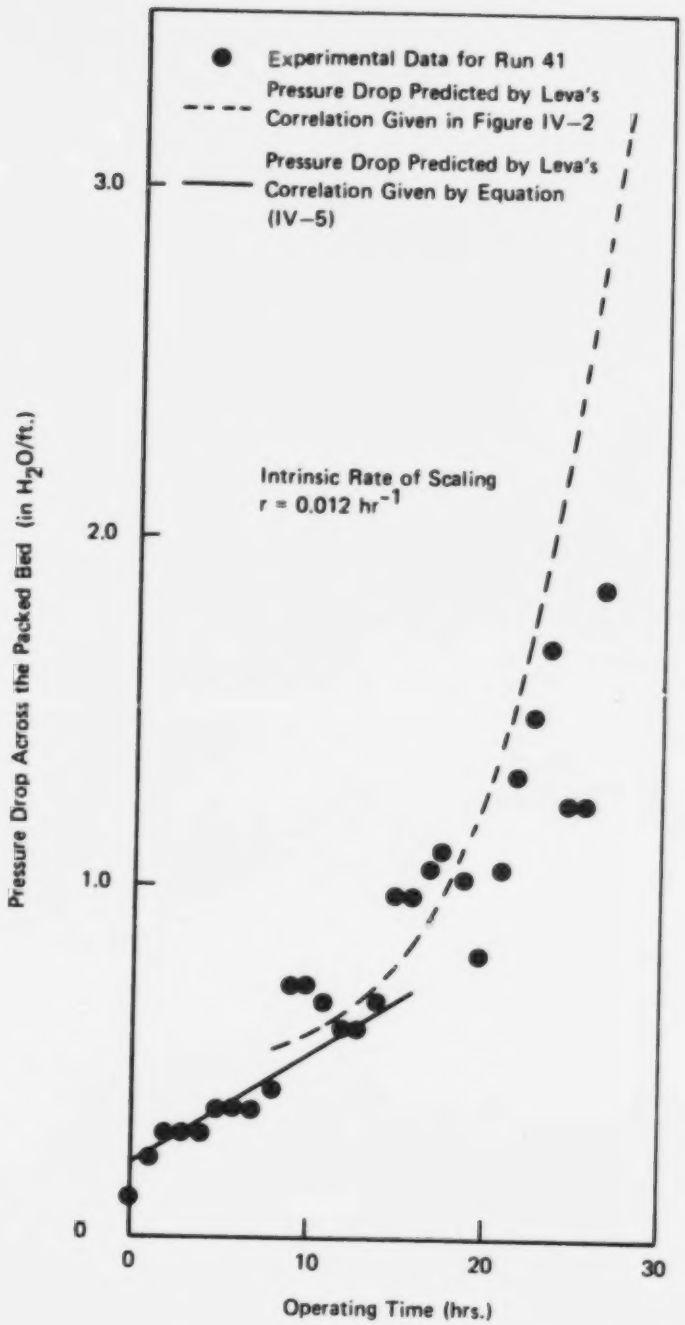

FIGURE IV–5 COMPARISON OF THE MEASURED PRESSURE DROP ACROSS THE PACKED BED WITH THE PRESSURE DROP PREDICTED BY STANDARD CORRELATIONS ASSUMING THE INTRINSIC RATE OF SCALING CONSTANT

$$\frac{\Delta P}{Z} = \alpha 10^{\beta L} \frac{G^2}{\rho_G} \qquad \text{(IV-5)}$$

Where $\frac{\Delta P}{Z}$ = the pressure drop per unit length of column (in. H_2O/ft),

G = Gass mass velocity, (lb./ft^3),

ρ_G = Gas density, (lb./ft^3)

L = liquid mass velocity,(lb,/sec ft^2),

and α and β are constants which depend on packing size and type. The constants α and β can be related to fractional voids as shown in Figures IV-6 and IV-7, respectively. Substituting these functional relationships of α and β into Equation IV-5, gives

$$\frac{\Delta P}{Z} = (15.0 - 19.0\varepsilon) \frac{G^2}{\rho_G} 10^{L(1.119-1.22\varepsilon)} \qquad \text{(IV-6)}$$

Since the void fraction ε is known as a function of time through Equations IV-3 and IV-4, the pressure drop can be calculated as a function of time using Equation IV-6 as shown in Table IV-2.

TABLE IV-2

Pressure Drop as a Function of Time on Line
Predicted by Equation IV-6 for Run 39

t,hr	$(\frac{\Delta P}{L})$ column, $\frac{\text{in } H_2O}{\text{ft.}}$	$(\frac{\Delta P}{L})$ Total, $\frac{\text{in } H_2O}{\text{ft.}}$
0	0.018	0.250
4	0.095	0.331
8	0.184	0.420
12	0.280	0.516
16	0.384	0.620

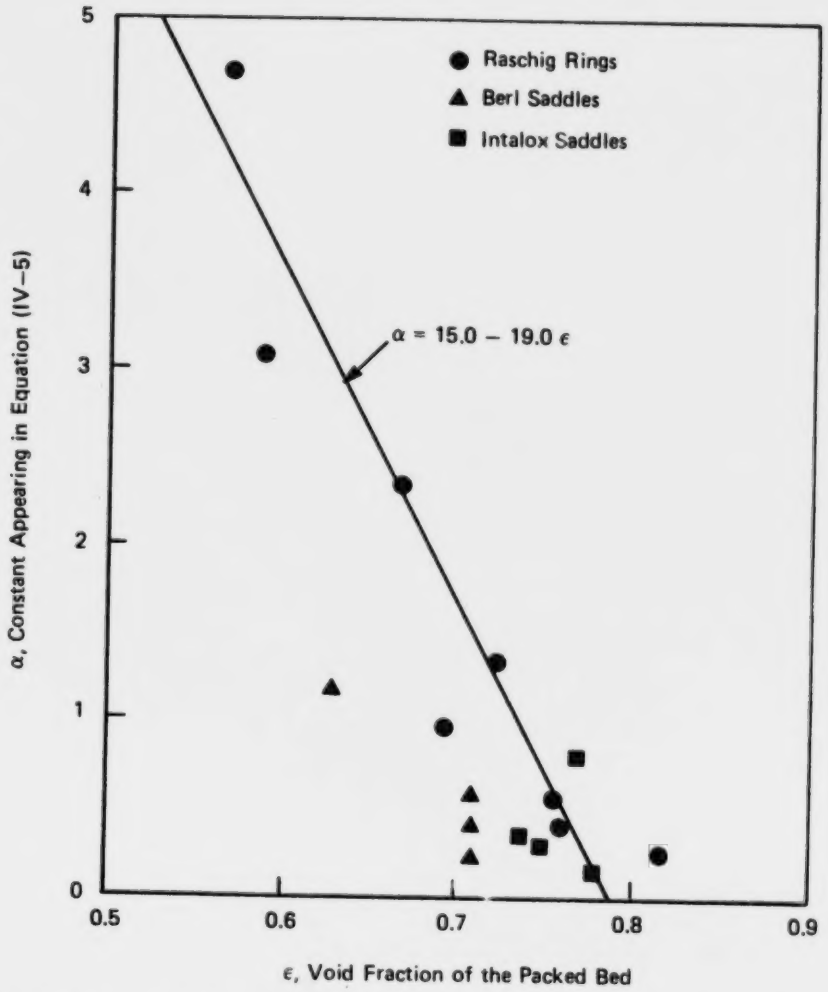

FIGURE IV–6 THE FUNCTIONAL RELATIONSHIP BETWEEN α, A CONSTANT APPEARING IN THE PRESSURE DROP CORRELATION FOR PACKED BEDS GIVEN BY EQUATION (IV–5) AND THE VOID FRACTION OF THE PACKED BED, ϵ

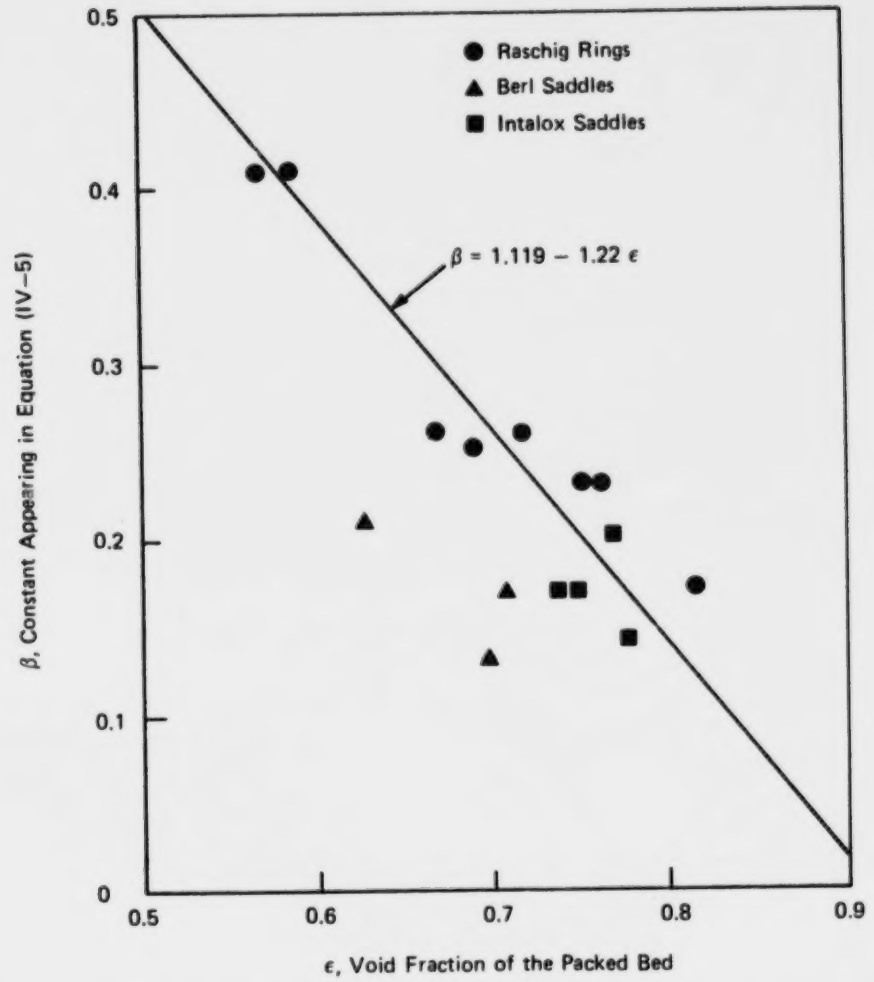

FIGURE IV–7 THE FUNCTIONAL RELATIONSHIP BETWEEN β, A CONSTANT APPEARING IN THE PRESSURE DROP CORRELATION FOR PACKED BEDS GIVEN BY EQUATION (IV–5) AND THE VOID FRACTION OF THE PACKED BED, ϵ

The total pressure drop as a function of time determined by correlation given by Equation (IV-5) is plotted as a solid line on Figures IV-3, IV-4 and IV-5. Again good agreement between experimental and predicted pressure drops can be seen.

Using standard pressure drop correlations for packed columns and assuming constant specific area of the packing and constant intrinsic rate of scale formation in the column appears to give good agreement between predicted and experimental pressure drops. The concept of intrinsic rate of scaling is therefore a useful measure of the scaling taking place under given operating conditions.

B. Experimental Results

1. pH Control

Preliminary experiments were carried out to determine the effects of mechanical deposition of solids in the packed bed scrubber by circulating a slurry of 15% solids content in the absence of sulfur dioxide or oxygen. From the increase in pressure drop across the column it was obvious that some solids deposition was occurring even in the absence of scrubbing or oxidation. However, with a 6% solids concentration the problem disappeared.

Further experiments were carried out to examine the extent of scaling in the presence of 5% calcium sulfate solid, but without oxygen in the flue gas to cause further oxidation. The process water was decanted from the solid and used to prepare fresh make up slurry to ensure that a saturated solution was maintained and simulate closed loop operation. Results from these runs are summarized in Table IV-3. With the inlet pH at 6.2 - 6.3 appreciable scaling was observed at 100°F and the rate was a factor of three higher at 125°F. Scaling at 125°F was much less when calcium sulfate was excluded from the slurry, suggesting that the presence of calcium sulfate is a factor in calcium sulfite scaling. However, when the stoichiometry was reduced (Run 33) to control the pH between 5.8 - 6.0 the scaling was reduced to about 15% of that observed at pH 6.2 - 6.3 (Run 31). Thus, pH control below pH 6 has a dramatic effect in reducing calcium sulfite scale, presumably because it allows much more of the sulfite to remain in solution minimizing precipitation in the scrubber. Operation at this lower pH has an adverse effect on efficiency. SO_2 removal is 15-20% lower but it also provides a lower stoichiometry and more efficient

TABLE IV-3 SUMMARY OF CALCIUM SULFITE SCALING DATA

2000 ppm P_{SO_2}, N_2 = 5 scfm, L/G = 50 Make-up used 85% Recycled Process Water

Run	Solid Conc.	Oxygen	pH Inlet	Time on Line (hrs)	Intrinsic Scaling Rate (hr^{-1})	Stoichiometry	Temp. (°F)	SO_2 Removal Efficiency (%)
30	5% $CaSO_4$ 1% $CaCO_3$	0	6.2-6.3	28	0.013	0.94	100	65-75 For pressure drop from 0.25 to 1.5 in. of water.
31	5% $CaSO_4$ 1% $CaCO_3$	0	6.15-6.3	9	0.045	0.94	125	60-75 For pressure drop from 0.25 to 2.0 in. of water.
32	5% $CaSO_3$ 1% $CaCO_3$	0	5.7-6.4	33	0.011	0.94	125	65-80 For pressure drop from 0.5 to 3.0 in. of water
33	5% $CaSO_4$ 0.5% $CaCO_3$	0	1) 5.8:0-20 hr 2) 6.0:20-38 hr 3) 6.3:38-58 hr 4) 5.8:58-72 hr	72	0.0067	0.42-0.65	125	45-55

Arthur D Little Inc

utilization of calcium carbonate. The loss in absorption efficiency can be counteracted by a change in scrubber design or by the use of additives with higher stoichiometry (described in Section 3).

2. Seed Crystals

If supersaturation is minimized by acceleration of the precipitation process away from the walls of the containing vessel, scaling can be avoided. In some systems, this can be achieved by seeding the solution with particles of a particular type, preferably of the same polymorph as the precipitating species. Nucleation and growth of crystallites is thereby enhanced, and precipitation is largely confined to the bulk of the solution. Even where crystallization occurs on the walls the deposits may be softer and easier to remove.

Seeding was one of the earliest scale control methods to be used in wet scrubbing plants, and is still applied more or less successfully in modern units. One of the first wet scrubbing systems for control of sulfur dioxide emissions from power plants was set up in Fulham, England around 1935. Blockage became severe enough to force a shut-down after 72 hours. (A scale 2-3 inches thick was found on portions of the scrubber surfaces). Hard deposits of pure gypsum were found in an area of the scrubber that had only been exposed to clarified liquor and it became clear that a crystallization phenomenon or chemical scaling was involved.

Lessing's work[2] showed that if supersaturation of calcium sulfate were to be limited in the scrubber, a high proportion of solids in the recirculating liquors was necessary to seed the crystallization adequately. Actual times for the desupersaturation of solutions which had the necessary slight degree of

supersaturation required to prevent scaling were longer than those found in the laboratory (with similar seed concentrations). The crystalline shape of the calcium sulfate was found to seriously limit the effectiveness of calcium sulfate seeding.

More recently, Research-Cottrell[3] found that an increase in slurry concentration from 2% to the 4-8% range helped to reduce scaling. The results were in part confirmed by TVA in their 4-8 cfm scrubber [9]. Circulation of 1% solids led to rapid scaling, while 4% solids helped to alleviate scaling. However, delay times were also different in the two cases. Mitsubishi[10] reports the use of seed crystals as one scale control measure, but does not present quantitative data on total solids or percentage of sulfite and sulfate in the scrubber liquor.

There are several practical difficulties in attempting to use seeding as an effective scale-control technique. These include:

a) Sludging and buildup of seed particles in stagnant zones--particularly with calcium sulfate hemihydrate

b) Change in the crystalline form of calcium sulfate over time, and an attendant loss of effectiveness.

c) Reduction of the efficiency of calcium sulfate seeds in the presence of calcium sulfite.

Seeding Experiments

To investigate the effects of calcium sulfate scaling, we used as a control run a carbonate slurry which was saturated with calcium sulfate, but contained no sulfate solid. The scrubber was operated at 125°F with 4% oxygen in the flue gas, and scaling was quite rapid causing shutdown of the unit in about 12

hours (Runs 36 and 45). The scrubber was also operated below pH 6 in order to minimize any possible calcium sulfite deposition. Experiments to show the effect of different seed crystals - gypsum, hemihydrate and anhydrite - are summarized in Table IV-4. With 1% gypsum seed crystals the scaling rate decreased to about 40% of that observed for the control run in spite of the fact that gypsum is not the thermodynamically stable form at 125°F. Concentrations of gypsum solid greater than 1% did not appear to reduce the rate of scaling much further, which is somewhat contrary to literature observations which suggest that the optimum is found in the range of 3-5% gypsum solids. It may be that a proportion of the seed crystals in prior work were inactive, due to aging or crystal form. Experiments were also carried out with calcium sulfate hemihydrate and anhydrite. Both of these were much worse than gypsum, and hemihydrate gave higher scaling rates than the control run.

TABLE IV-4 SUMMARY OF CALCIUM SULFATE SEEDING DATA

2000 ppm P_{SO_2}, N_2 = 5 scfm, 4% O_2, L/G = 50, 85% Recycled Process Water

Run	Solid Conc.	Additive	pH inlet	Time on Line (hrs)	Intrinsic Scaling Rate (hr^{-1})	Stoichiometry	Temp, (°F)	SO_2 Removal Efficiency (%)
36	Sat. soln $CaSO_4$ 0.5 $CaCO_3$	None	5.6-6.0	12.25	0.027	0.5-0.75	125	45-55
37	1% $CaSO_4$ 0.5% $CaCO_3$	Seed crystal gypsum	5.6-6.0	37	0.0086	0.5-0.8	100	50-60
35	1% $CaSO_4$ 0.5% $CaCO_3$	Seed crystal gypsum	5.6-6.0	32	0.0111	0.5-0.65	125	40-50
40	1% $CaSO_4$ 0.5% $CaCO_3$	Seed crystal Hemihydrate	5.6-6.0	15	0.036	0.4-0.6	125	45-55
46	1% $CaSO_4$ 0.5% $CaCO_3$	Seed crystal Anhydrite	5.6-6.0	16	0.0200	0.45-0.55	125	45-55

Arthur D Little Inc

3. ADDITIVES

Threshold additive treatment, although poorly understood, has become the most common scale control method used in contemporary desalination processes. Basically, it has been found that small quantities of certain polymeric electrolytes inhibit scale growth when present in far less than stoichiometric amounts. Although many fundamental studies have been carried out, the mechanism of scale control by threshold addition has never been adequately explained (and more than one mechanism may be operative).

Phosphate Additives

Sodium hexametaphosphate (Graham's Salt) was one of the first additives successfully used to treat boiler scale. It is known that hexametaphosphate addition greatly increases the negative mobility of the calcium ion, as though strongly negatively charged complexes were formed. However, the effective dose of hexametaphosphate is far too low for a sequestering mechanism to be tenable. It has been shown that surfaces treated with hexametaphosphate retain their scale retarding properties even when contacted with supersaturated carbonate solutions not containing the phosphates. This evidence, combined with the observation that crystals formed in the presence of hexametaphosphate are distorted in structure, suggests a surface absorption mechanism in which crystal nucleation and growth is inhibited.

Organic Additives

A range of acrylic acid homopolymers and copolymers was synthesized and tested for alkaline scale suppression in a pilot plant evaporator (at around 3 ppm). With a polymer of this type containing 66% acrylic acid,

it was shown by using conductance measurements to follow ionic concentration, that the mechanism of scale suppression was an interference with crystallization kinetics which results in a modified crystal habit. During the evaporation of calcium sulfate solutions in beaker tests, specific conductance increased as the concentration rose, but then fell rapidly as the scaling rate exceeded the rate of concentration of the solution. Four ppm was sufficient to extend the period for initiation of significant precipitation from 10 minutes to 25 minutes. The presence of the polymer (at 3 and 4 ppm) introduces an induction period in the scaling rate which radically decreases the rate of crystallization. Thus, the effect of the additive is to hold calcium sulfate in solution at levels well above the equilibrium solubility limit in the absence of the additive.

The deposits formed in the presence of polymeric additives generally have a rather large organic content. This suggests considerable attrition of additive material and hence an increase in additive costs. Reports that acrylic-based polymers yielded self-cleaning scales are found to be probably dependent on the presence of small amounts ($\sim$0.2 ppm of aluminum, magnesium or zinc.)

Scales formed in the presence of both polyelectrolytes and the metal ions above were found to strip easily from the copper surfaces of a laboratory spray evaporator on exposure to air. The lower molecular weight materials in the range 1000-16000 were most effective. This work indicates how sensitive scale formation is to precise operating conditions particularly with respect to trace impurities in the system.

Selection of Additives for Preliminary Screening

Based on previous experience with anti-scaling additives and consultation with vendors, the phosphate and polymeric additives listed in Table IV-5 were selected for initial screening. Each of the additives selected has proven effective in controlling scaling in particular types of lime systems. Nine of the additives listed are proprietary products and their physical properties are described in Appendix 5. The remaining four additives are commonly available chemicals.

Sodium hexametaphosphate $(NaPO_3)_6$, a so-called glassy phosphate, is a widely used constituent of commercial inhibitors for controlling carbonate scale in potable water treatment. Sodium pyrophosphate is reported to be the major scale inhibiting constituent in multi-stage distillation plants in Kuwait. A combination of sodium silicate and sodium hexametaphosphate has proven to be more effective in reducing deposits in potable waters than either material alone. Sodium tripolyphosphate is one of the constituents of PD-8, and has been used widely for scale control in desalination operations.

Initial Screening Tes'

Initial exploratory experiments were conducted with the objective of developing conditions which lead to significant and reproducible scaling so that anti-scaling additives might be assessed in a quantitative manner. Details of the apparatus and test results are presented in Appendix 2.

In addition to the initial slurry composition, several other variables which may affect the rate of scaling have been identified. These are: the rates of addition of SO_2, oxidants and sulfuric acid, temperature, residence time in the reacting area, and the type of surface. Since an exhaustive investigation of

TABLE IV-5

ANTI-SCALING ADDITIVES SELECTED FOR PRELIMINARY SCREENING

Trade Name	Manufacturer	Type of Additive
Lime Treet	Dearborn Chemical Division W.R. Grace and Company	Mixture of alkaline material and a synthetic non-ionic organic polymer
Acrysol A-1	Rohm and Haas Company	Polyacrylate, MW> 50,000
Acrysol A-3	Rohm and Haas Company	Polyacrylate, MW>150,000
Acrysol A-5	Rohm and Haas Company	Polyacrylate, MW>300,000
Calnox 214 DN	Aquaness Chemical Co. Houston, Texas	Aqueous solution of polyacrylate, MW ≈ 750
Darex 40	W.R. Grace and Company Cambridge, Mass.	Sodium polymethacrylate
Dequest 2000	Monsanto Company St. Louis, Missouri	Phosphoric acid analog of EDTA (ethylenediamine tetracetic acid)
PD-8 (formerly Hagevap LP)	Bull & Roberts, Inc. 785 Central Avenue Murray Hill, N.J.	Mixture of sodium tripoly-phosphate, lignin sulfonate, and an anti-foaming agent.
Sodium hexa-metaphosphate		
Calgon CL-14	Calgon Company	Liquid organic formulation, containing a proprietary polymer and an organic phosphorous compound.
Sodium Pyrophosphate		
Versenex 80	Dow Chemical Company	Aqueous solution of pentasodium diethylenetriaminepentacetic acid
Quadrol	Wyandotte Chemicals Co.	N, N, N^1, N^1-tetrakis (2-hydroxypropyl)-ethylenediamine
10 ppm Metso and 10 ppm sodium hexametaphosphate		Mixture of sodium silicate (Metso) and sodium hexametaphosphate
Sodium tripoly-phosphate		

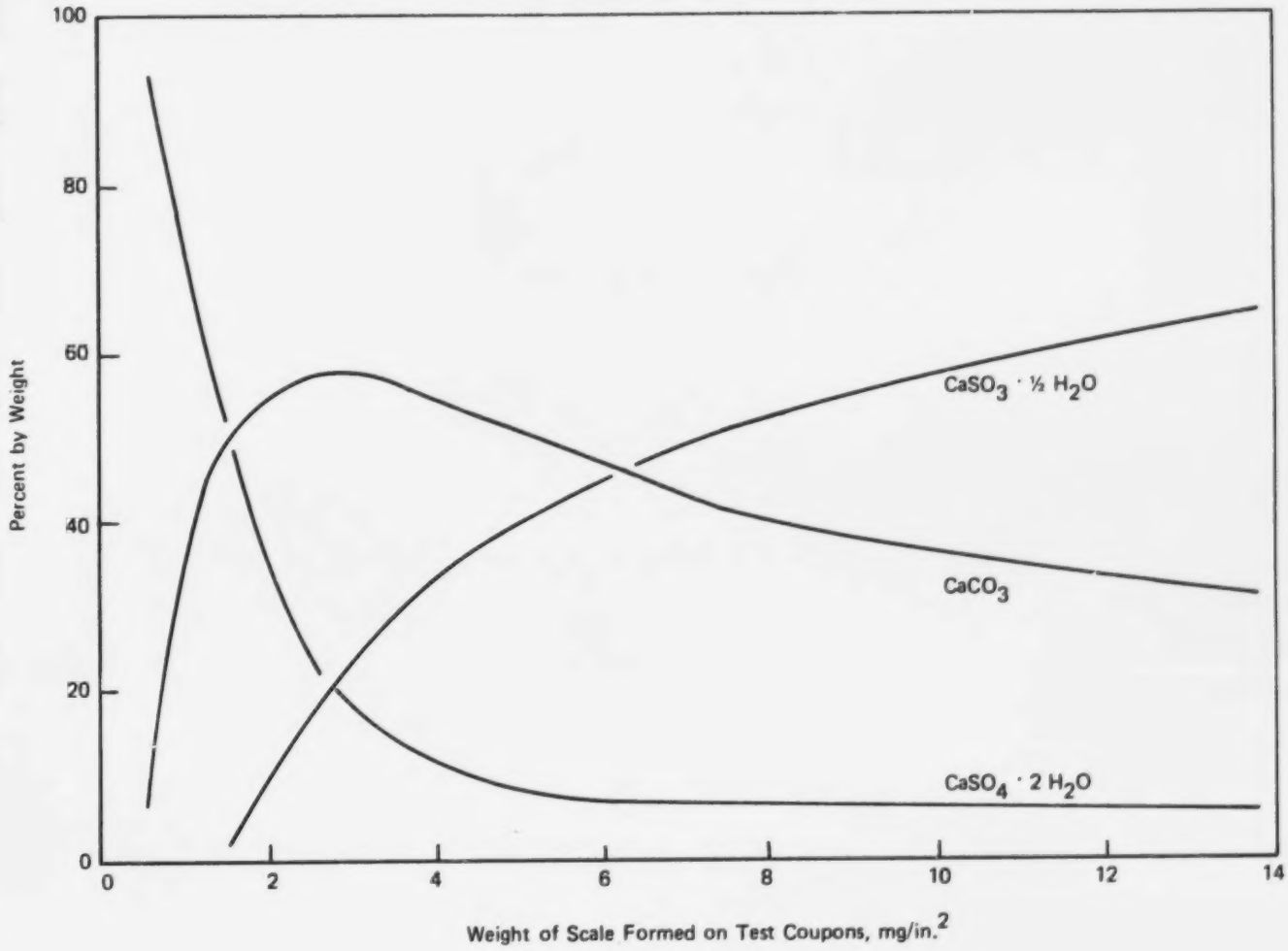

FIGURE IV–8 SCALE ANALYSIS VERSUS SCALE WEIGHT

all these variables at several levels is impractical in screening tests, those combinations which seemed from experience most likely to produce rapid and reproducible scaling were chosen.

Preliminary experiments with panel materials showed that mild steel and brass were attacked by the acidic slurry, and that little scale formed on Teflon. However, since the primary concern was with anti-scaling additives, subsequent tests were limited to panels of 304 stainless steel and PVC coated mild steel, both of which collected scale deposits without corrosion.

Lime Treet, and Acrysol A-3 and A-5 were found to have definite negative effects resulting in increased scaling. However, Lime Treet was selected for bench-scale testing to provide a point of comparison.

Darex, Versenex 80, Quadrol, sodium silicate-sodium hexametaphosphate, sodium pyrophosphate and sodium tripolyphosphate exhibited small effects (either positive or negative) and were felt to be of little use compared to the more promising additives examined in the bench scale scrubber.

X-ray Analysis/Scale Deposits

The X-ray diffraction analyses of scale deposits removed from coupons in the screening runs show a general trend in composition as a function of thickness, noted graphically in Figure IV-8. As a rule, sulfate deposits appear first as the scale is initially formed and until it grows to a certain thickness (<1 mg/in^2). Carbonate and then sulfite deposit after this thickness has been reached. The deposition of calcium carbonate, which is not normally found in bench scale or full scale scrubber experiments is probably due to the use of a very large excess of carbonate in the screening experiments. Thus, the growing scale appears

to collect carbonate solid from the slurry. As the scale thickness increases, sulfite scale predominates with some carbonate deposition and essentially no further sulfate deposition. This suggests that sulfate is an important precursor or initiator of overall scale formation.

Bench Scale Scrubber Tests

Five of the more promising additives identified in the screening program were tested under conditions of the control run which was conducive to high rates of calcium sulfate scaling. Results in Table IV-6 show that the qualitative agreement between the screening and bench scale scrubber tests are quite good. Details of the bench scale scrubber tests are summarized in Table IV-7. One additive "Lime Treet" was found to give poor results as it did in the screening experiments and the run was terminated. All the other additives showed improvements over the control run. Dequest 2000 and PD-8 were both tested at two concentrations, sodium hexametaphosphate at one concentration. These three additives tended to lower the pH which was compensated by increasing stoichiometry (with a consequent improvement of 15-20% in SO_2 removal efficiency). The best additives found were Calnox 214 DN and Calgon CL-14 which reduced the rate of scaling by almost 75% of that observed in the control experiment. Again, a buffering effect and improvement in SO_2 removal efficiency was observed with these two additives. Calnox 214 DN was tested at three concentrations. The highest concentration, 0.25 ml/l was found to be the most effective. A synergistic effect was also found when Calnox additive was used with gypsum seed crystals. The scaling was further reduced although it was observed that 3% gypsum showed a higher rate of scaling than the 1% gypsum slurry.

Table IV-6 COMPARISON OF ANTI-SCALING ADDITIVES IN SCREENING AND BENCH-SCALE SCRUBBER TESTS

Additive	Hours of Scrubber Operation	Scale Weight mg/in^2 (screening tests) PVC	S. Steel	Type of Additive
Calnox 214 DN	48.5	1.4	2.0	Sodium polyacrylate (M.W. about 750) + lignosulfonates
Calgon CL-14	44.5	3.5	2.2	Aminomethylenephosphorate (AMP)
Sodium hexametaphosphate	31	0.6	0.8	
PD-8	27.5	1.5	0.9	Sodium tripolyphosphate + lignosulfonates
Dequest 2000	20	0.7	0.8	Polyacrylate
None (control)	12.25	7.5*	7.2*	-
Lime Treet	3	22.6	11.8	Synthetic Polymer

* average of 3 runs.

TABLE IV-7 SUMMARY OF ADDITIVE DATA

2000 ppm P_{SO_2}, N_2 = 5 scfm, 4% O_2, L/G = 50, 85% Recycled Process Water

Run	Solid Conc.	Additive	pH Inlet	Time on Line (hrs)	Intrinsic Scaling Rate (hr^{-1})	Stoichiometry	Temp. (°F)	SO_2 Removal Efficiency (%)
45	Sat. soln $CaSO_4$ 0.5% $CaCO_3$	None	5.6-6.0	13	0.0246	0.5-0.7	125	50-60
38	Sat. soln $CaSO_4$ 0.5% $CaCO_3$	Dequest 2000 (.005, .05 ml/1)	5.6-6.0	20	0.0174	0.6-1.4	125	55-70
39	Sat. soln $CaSO_4$ 0.5-1.0% $CaCO_3$	Sodium hexameta-phosphate (0.02 g/1)	5.6-6.0	31	0.011	0.6-1.2	125	50-70
41	Sat. soln $CaSO_4$ 0.5-1.0% $CaCO_3$	PD-8 (0.02, 0.04 g/1)	5.6-6.0	27.5	0.0124	0.7-1.4	125	60-75
42	Sat. soln $CaSO_4$ 0.5-1.0% $CaCO_3$	Calnox 214 DN (0.025 ml/1)	5.6-6.0	48.5	0.0071	0.6-1.0	125	60-70
43	Sat. soln $CaSO_4$ 0.5% $CaCO_3$	Calgon CL-14 (0.05 ml/1)	5.6-6.0	44.5	0.0077	0.6-0.80	125	55-70
44	Sat. soln $CaSO_4$ 0.5% $CaCO_3$	Lime Treet (0.005 g/1)	Lime Treet, insoluble in alkaline solution. Run terminated after 3 hours due to excessive settling of solids.					
47	Sat. soln $CaSO_4$ 1% $CaCO_3$	Calnox 214 DN (0.01 ml/1)	5.6-6.0	19.5	0.0164	0.65-0.85	125	60-70
48	Sat. soln $CaSO_4$ 1% $CaCO_3$	Calnox 214 DN (0.017 ml/1)	5.6-6.0	22	0.0145	0.4-0.7	125	45-65
49	1% $CaSO_4$ 1% $CaCO_3$	Gypsum Calnox 214 DN (0.05 ml/1)	5.6-6.0	70	0.00457	0.6-0.9	125	55-65
50	3% $CaSO_4$ 1% $CaCO_3$	Gypsum Calnox 214 DN (0.1 ml/1)	5.6-6.0	51.5	0.00622	0.8-0.9	125	55-70

Arthur D Little Inc

C. Implications of the Scaling Model for Scrubber Operation

The scaling model works quite well for the packed bed scrubber and it should be possible to extend this model to other types of scrubber. For example, an intrinsic scaling rate for the TCA pilot plant scrubber can be estimated from the time to catastrophic scaling and the change in void fraction of the grid using Equation IV-3:

$$-r = \frac{\varepsilon - \varepsilon_o}{t - t_o} \text{ hrs}^{-1}$$

Similarly the time to catastrophic scaling can be estimated by using an appropriate form of the Leva correlation to relate pressure drop to void fraction. Changes in pressure drop can then be used to define intrinsic rates of scaling and predict the time on line before flooding of the column occurs due to scale build-up.

V. SULFITE OXIDATION

A. Introduction

Scale formation incorporating calcium sulfate is a major problem in limestone wet scrubbers due to the oxidation of calcium sulfite to calcium sulfate by oxygen in the flue gas. The extent of oxidation in different scrubbers is quite variable and the conditions controlling oxidation and the reaction mechanism are not well understood. Oxidation of calcium sulfite under controlled laboratory conditions has not been widely studied although a related reaction, oxidation of sodium sulfite, has been extensively investigated. However, in spite of this detailed study over many years, the mechanism of the latter reaction is still not completely understood,although it appears to be very rapid, and mass transfer effects can be important. Most literature data refer to oxidation of relatively concentrated sodium sulfite solutions in alkaline solutions, whereas the present interest is in oxidation of sulfite in calcium carbonate/calcium sulfite slurries at neutral or acid pH.

The objectives of this limited present program were:

1. to investigate the variables controlling the oxidation of dilute sodium sulfite solutions, particularly as a function of pH.
2. to investigate the variables controlling the oxidation of calcium sulfite using the previous results as a baseline.

A continuous stirred tank reactor (CSTR) was chosen to carry out the experiments because this type of reactor is simpler to treat in terms of the kinetic expressions, although the interfacial contact area between the liquid and gas phases is not well defined. Our experiments with sodium sulfite were intended to provide an appropriate baseline which could be compared with literature data and with the calcium salt data.

Absorption in Stirred Vessels

It is possible to distinguish three separate regions of overall absorption rate characterized by the dependence of the reaction rate on the rate of stirring, or rate of impeller rotation. Figure V-I shows these three zones. In Region 1 the oxidation rate is slow and strongly dependent on the gas flow rate, essentially independent of the agitation rate. In Region 2 the oxidation rate is increasing rapidly; the agitation rate is more important and the gas flow rate is of less importance. In Region 3 the reaction rate has become independent of both agitation rate and gas velocity. The mass transfer rate, therefore, has been increased by the intensity of agitation, until it has become equal to, or faster than, the chemical reaction rate. At this point, the chemical reaction is rate-controlling, and the overall rate can be increased only by changing factors such as temperature, catalyst concentration and reactant concentration, which would increase the chemical reaction rate.

It is possible to distinguish the system under mass transfer control from that of the chemical reaction rate control by measuring the overall reaction rate under conditions of varying impeller speed, gas flow rate, and reactant concentration. For the system under mass transfer control, gas absorption rates will be strongly dependent on agitation rate, on gas partial pressure, and perhaps on gas flow rates, and will be substantially independent of temperature and reactant concentration.

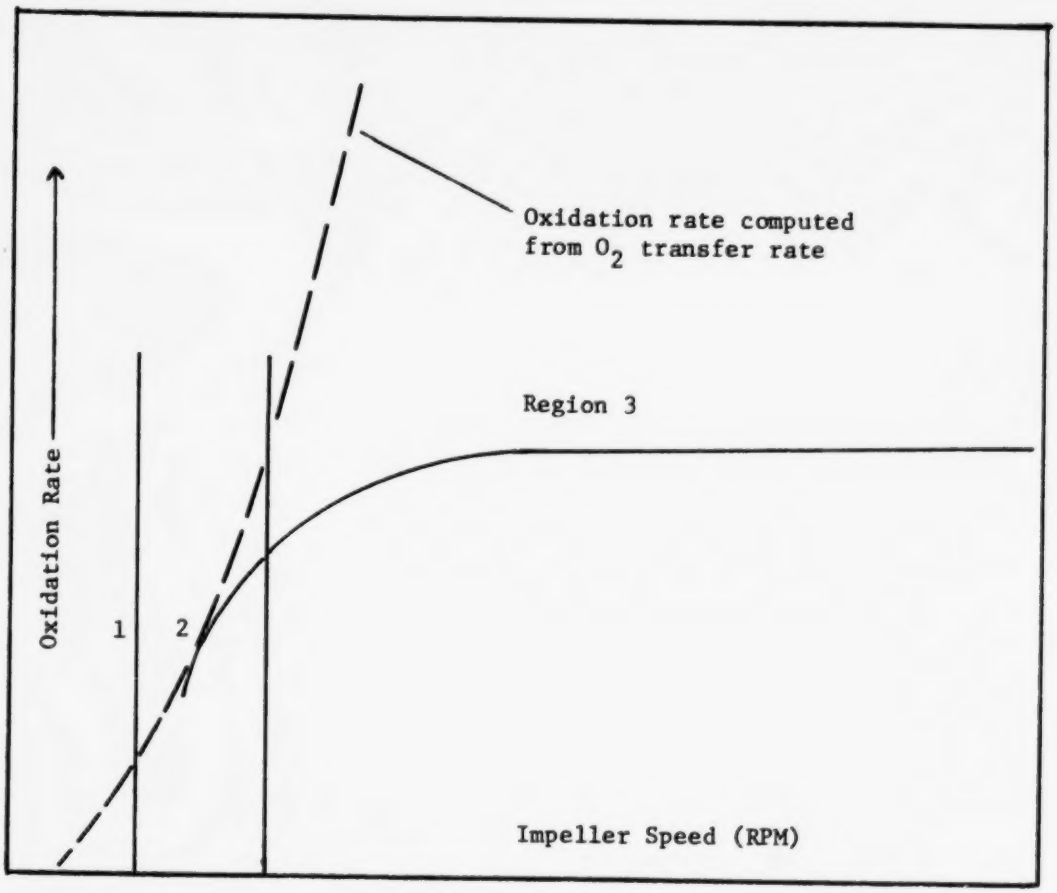

Figure V-1 Oxidation Rate vs. Impeller Rotation
(A Representative Curve for a Stirred Vessel).

B. Evaluation of Literature Data on Sodium Sulfite

A detailed comparison of the results with available literature data is difficult because of the wide range of techniques and reaction conditions employed by other workers. We have reexamined much of the literature data and tried to assess its salient characteristics relative to the work in progress. Much of the literature is concerned with use of the reaction to determine mass transfer characteristics in various types of equipment, rather than the basic kinetics of the reaction. Therefore, these experiments tend to concentrate on higher oxygen concentrations (air) and relatively high sulfite concentrations.

Reaction Order

When sulfite is present in a large excess, then the reaction might be expected to become proportional to some power of the oxygen concentration but independent of sulfite concentration. The reverse should be true when oxygen is in large excess and the rate can become proportional to the sulfite concentration. In reality, these represent limiting cases and the reaction order becomes variable and much more complex. Fractional orders are possible due to changes in the potential rate controlling steps. For the heterogenous reaction of oxygen (gas) with sodium sulfite solution in a continuous stirred tank reactor, the situation is further complicated by the mass transport limitations. These include absorption of oxygen into the liquid and diffusion of oxygen and sulfite ions in the liquid phase. The process of oxygen absorption is itself complex and is dependent on such parameters as gas flow rate, oxygen partial pressure, vessel design and the interfacial area between the gas and liquid phase. The latter is controlled by the impeller design and speed of rotation.

We have summarized in Table V-1 the literature data showing the order of reaction and the range of reaction conditions under which these parameters were measured. It can be seen that the results vary between 0 and 2 for both oxygen and sulfite ion. The range of sulfite concentration studied varies from 1 to 10^{-3} moles per liter. However, in general the results follow the expected direction. For example, Astarita[2] found the reaction was second order in oxygen at high sulfite concentrations and zero order at low sulfite concentrations. Most workers found that the reaction was first order with respect to sulfite, but at high sulfite concentrations (>0.5 mole/l) the reaction rate becomes zero order in sulfite. At the other extreme, Rand and Gale[5] found the reaction approximately second order in sulfite at very low sulfite concentrations (10^{-3} mole/l).

Most of the literature data refers to reaction with air (i.e., dissolved oxygen in equilibrium with air). We are concerned with a much lower oxygen partial pressure (4%); this would tend to make the overall reaction rate more dependent on the oxygen absorption rate. However, the range of sulfite concentration of interest is also somewhat lower than the ranges previously investigated. Thus, it is difficult to predict, a priori, from the literature data, what the

pH Effects

Data in the literature,[5,7] although not comprehensive, indicate that the overall oxidation rate of sodium sulfite decreases with pH. There is disagreement on the magnitude of the effect; however, if should be noted that the two authors used widely different measuring techniques.

TABLE V-1 SUMMARY OF LITERATURE DATA ON REACTION ORDER

Reference	$SO_3^=$ Conc. mole/ℓ	O_2 Conc. mole/ℓ	Reaction Order $SO_3^=$	Order O_2
Reith[1]	0.8		0	2
Astarita et al[2]	.06			0
	.25			1
	.25-1.0			2
De Vaal & Okeson[3] (catalized)	0.8		1	
Srivastava et al[4]	>0.4	$6 - 24 \times 10^{-4}$	0	1
Rand & Gale[5]				
pH 6.5-7.7	10^{-3}	DO>0.8 Mg/ℓ	2.3	0
pH 4.2-6.4	10^{-3}	(in ≡ with air)	1	
Cooper et al[6]	0.1-1		1	
Fuller & Christ[7]	$<1.5 \times 10^{-2}$	Sat. soln.	1	0
Westerterp et al[8]	0.02		0	1
(catalyzed)	0.01		1	0

C. Experiments with Sodium Sulfite (Mass Transfer Effects)

The literature data of Cooper, Fernstrom and Miller[6] on the oxidation of sodium sulfite in aqueous solution catalyzed by cobalt naphthenate found that there was no evidence of chemical reaction rate control, even up to fairly high agitation power inputs. The overall reaction rate was independent of sulfite or sulfate concentration, and strongly dependent on agitation rate and gas flow rate.

All the data we have obtained for sodium sulfite also appeared to show the reaction was dependent on impeller rotation rate, even at the highest rates (~700 rpm), obtainable in the apparatus, although there is perhaps some indication that we are close to the chemical reaction rate limit in a few experiments (e.g., the data in Figure 5, Appendix 2).

As further confirmation, we have used the equation proposed by Westerterp and co-workers[8] to find what they define as the "critical impeller speed". Westerterp and co-workers have shown that there is a critical impeller speed below which both gas velocity and impeller speed will affect the mass transfer coefficient. Above this critical impeller speed the mass transfer coefficient is independent of the gas velocity. This critical impeller speed is defined by η_o in the equation shown below. It is notable that η_o, defined by:

$$\eta_o D = [\sigma g/p]^{0.25} [A + G (T/D)]$$

where D = impeller diameter, ft.

$[\sigma g/p]^{0.25}$ = 1950 ft/hr. for water at 25°C

A + B are constants and functions of impeller shape, for a flat bladed turbine A = 1.22, B = 1.25

T = Tank diameter, ft.

is usually quite high and calculation from this equation gives a value in our apparatus of η_o = 726 rpm. This is approximately the upper limit of rotation rate in the present apparatus; therefore, all the results obtained are below this critical impeller speed, and should be a function of the gas velocity and impeller speed.

On this basis, our results should be comparable with the work by Cooper, et al.,[6] in a batch stirred tank reactor with a similar configuration to the present equipment. Using their data (stirring speed of 600 rpm, sodium sulfite concentration = 0.1 moles/l, oxygen concentration = 21%), we derive a mass transfer coefficient, $K_g a = 1.92 \times 10^{-2}$ lb moles/ft^3 hr. atm.

From the equation below, derived from Cooper's and other data, we can calculate the absorption (or oxidation) rates to be expected in our apparatus.

$$K_g a = 6.6 \times 10^{-6} \, V_G^{0.67} \, (P/V_L)^{0.76}$$

where

V_G = superficial gas velocity in vessel ft/hr. (based on empty cross section)

P = power input to liquid gas mixture in vessel from impeller, ft lb f/min.

V_L = volume of liquid in vessel, cu ft.

The calculated values are shown in Table V-2, together with the measured oxidation rate. It can be seen that the measured values are higher than the calculated values by a factor of 2, reasonable agreement considering the differences in apparatus and experimental technique. The equation also predicts the increased oxidation rate due to higher gas flow rates at 4% oxygen.

TABLE V-2 COMPARISON OF CALCULATED AND MEASURED OXIDATION RATES

Oxygen %	Gas Velocity ft^3/hour	Rate of Oxidation (lb moles/ft^3 hr) Calculated	Measured
4	30	0.57×10^{-3}	1.3×10^{-3}
20	30	2.8×10^{-3}	5.2×10^{-3}
4	60	1.0×10^{-3}	2.0×10^{-3}

TABLE V-3 EFFECT OF GAS FLOW RATE ON OXIDATION RATE

Nominal Sulfite Concentration (mmoles/ℓ)	Oxygen Concentration %	Oxidation Rate at 10 ℓ/min Compared with 5 ℓ/min
10	4	no difference
50	4	higher at 10 ℓ/min
100	4	higher at 10 ℓ/min
50	20	no difference
100	20	no difference

All the experiments were dependent on the impeller speed, but not all experiments were found to be dependent on gas flow rate. Results which were obtained for different solutions are summarized in Table V-3.at gas flow rates of 5 liters/minute and 10 liters/minute respectively. With 20% oxygen in the gas stream and nominal inlet concentrations of 0.1 molar and 0.05 molar sulfite solution no effect of gas flow rate was observed. A significant difference was observed for the same two sulfite concentrations at 4% oxygen in the gas stream; however, when the sulfite concentration was reduced to 0.01 molar with 4% oxygen, then no effect of gas flow rate was observable.

Effect of Oxygen Concentration

Thus, the experiments with sodium sulfite have shown that even at low oxygen concentration in the gas phase, equivalent to flue gas, and low concentrations of sulfite in solution, the reactions may still be mass transfer controlled. Therefore, one would expect the reactant concentration, temperature, and catalyst concentration to have little or no effect on the overall reaction rate. Certainly, the oxygen partial pressure in the gas phase must be considered one of the most important variables. Experiments were carried out [Figure 3, Appendix 2] up to 40% oxygen which did not show any limit to the reaction rate in sodium sulfite solution.

The experiments showed that the data could be represented on a log-log plot (Figure V-2) by the equation below,

$$R_{ox} = 78.7 \times 10^{-6} [P\ (O_2)]^{1.24} \text{ moles/l.sec)}$$

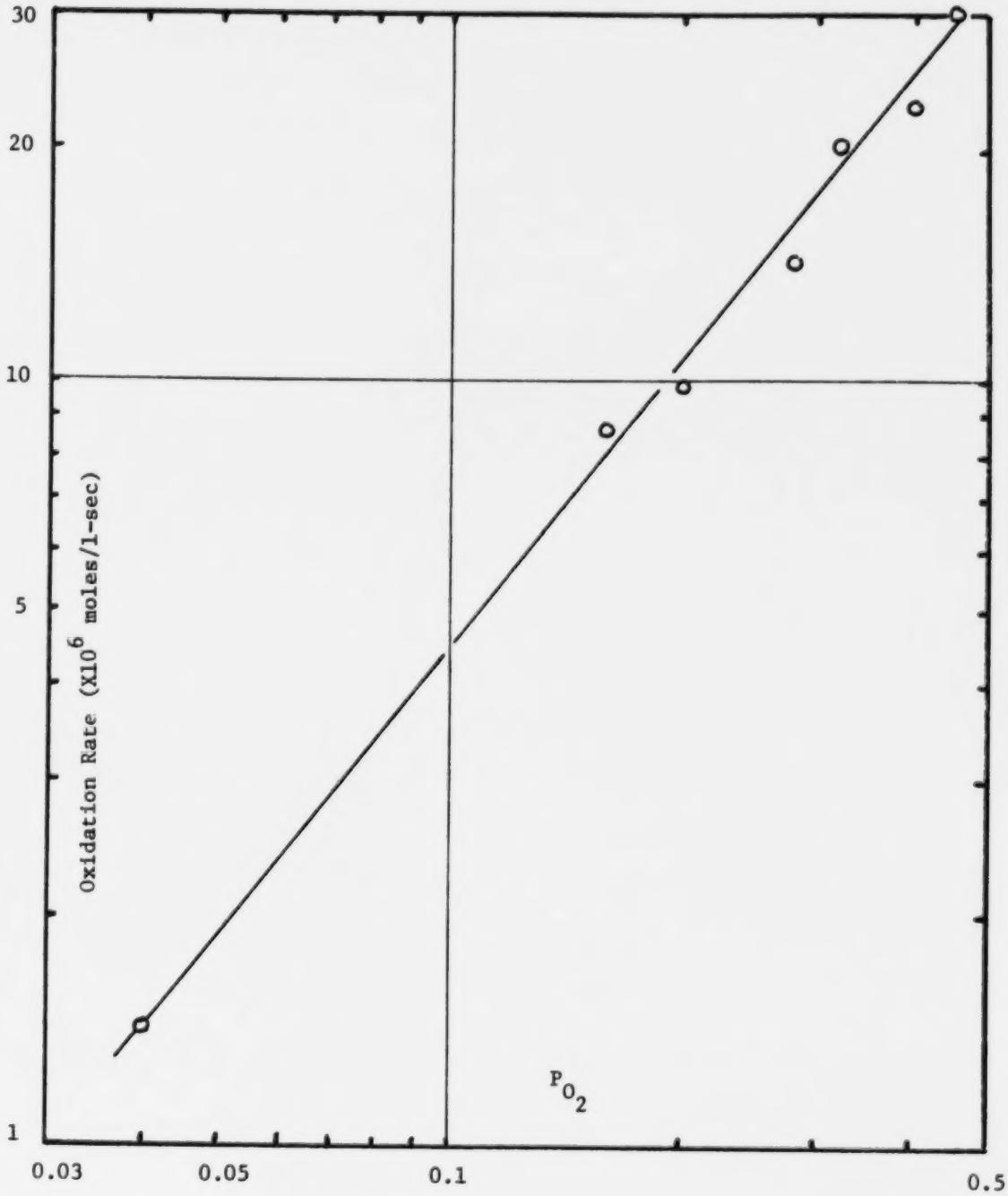

Figure V-2. Log Oxidation Rate vs. Log Partial Pressure of Oxygen for 400 mmoles/l Na_2SO_3 Feed (Impeller Rotation = 375 RPM)

showing that the data is approximately proportional to the oxygen concentration, although apparently not an integral number. This suggests that oxidation could be more rapid in the hold tank where the liquid is in contact with 20% oxygen, than in the scrubber where it is only in contact with the 4% oxygen present in the flue gas.

Effect of pH

Data on the oxidation rate of sodium sulfite as a function pH (changed by sulfuric acid addition)was plotted to evaluate the effect of hydrogen ion concentration and/or sulfite concentration. Although the change in oxidation rate as a function of pH is quite noticeable, in terms of hydrogen ion concentration, it leads to a relatively low exponent. It can be seen in Figure V-3 that the oxidation rate is inversely proportional to hydrogen ion concentration over the range from pH 9 to pH 3. There is no sign of any upturn at the lower end of the curve.

Effect of Impeller Speed

These data were then combined with the data showing the effect of impeller speed (I) at various sulfite concentrations. It was found that all this data could be consistently expressed by the equation given below (Figure V-4) which shows that the oxidation rate is proportional to impeller speed and inversely proportional to hydrogen ion concentration (or perhaps directly proportional to hydroxyl ion concentration). It was found that the most consistent set of

$$R_{OX} = 3.1 \times 10^{-10} [I]^{1.12}/[H^+]^{0.12}$$

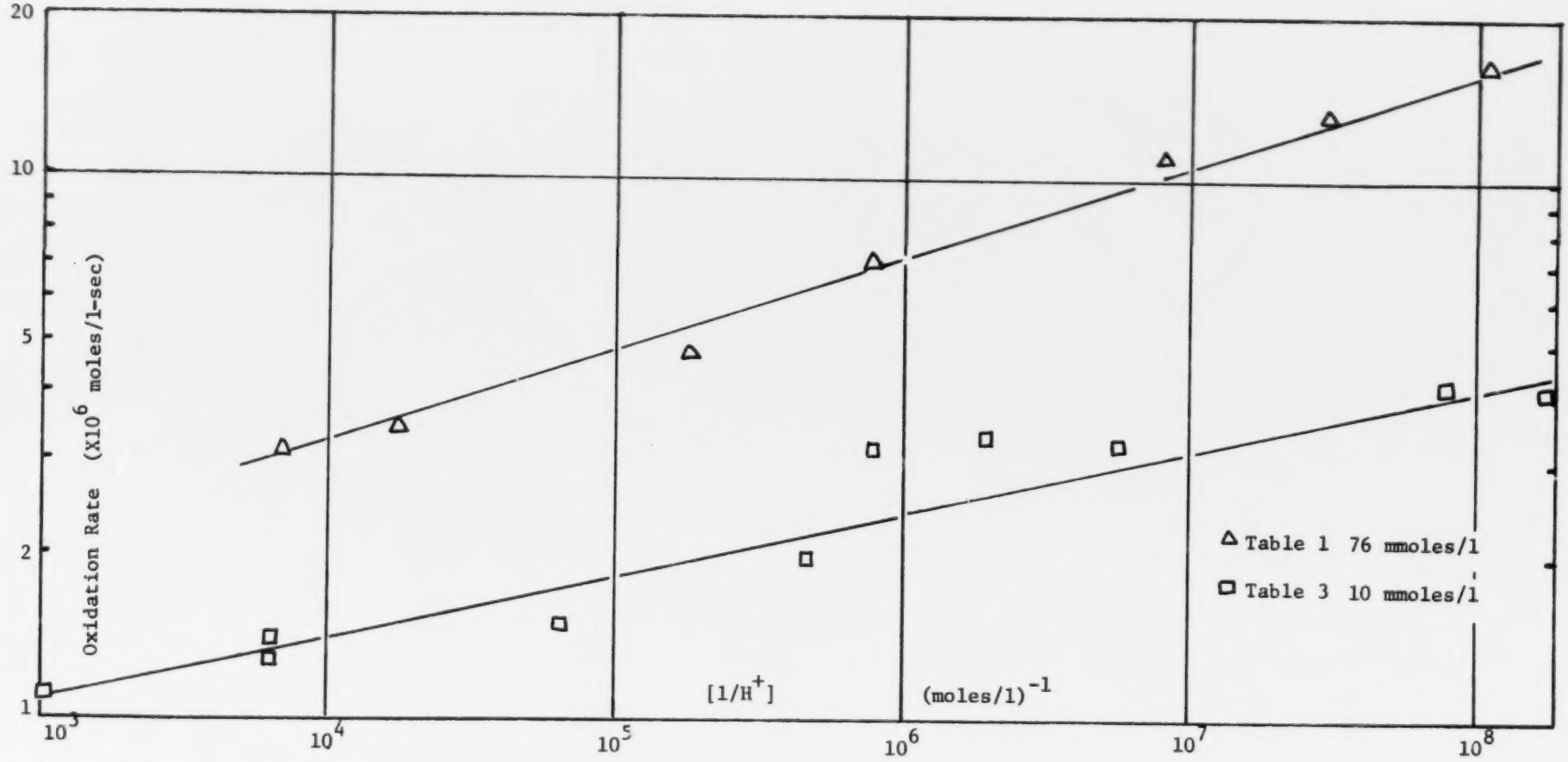

Figure V-3. Log Oxidation Rate vs. Log $[1/H^+]$ for Na_2SO_3 Feed at 4% Oxygen (Impeller Speed = 600 RPM), Tables 1 and 3.

Arthur D Little Inc

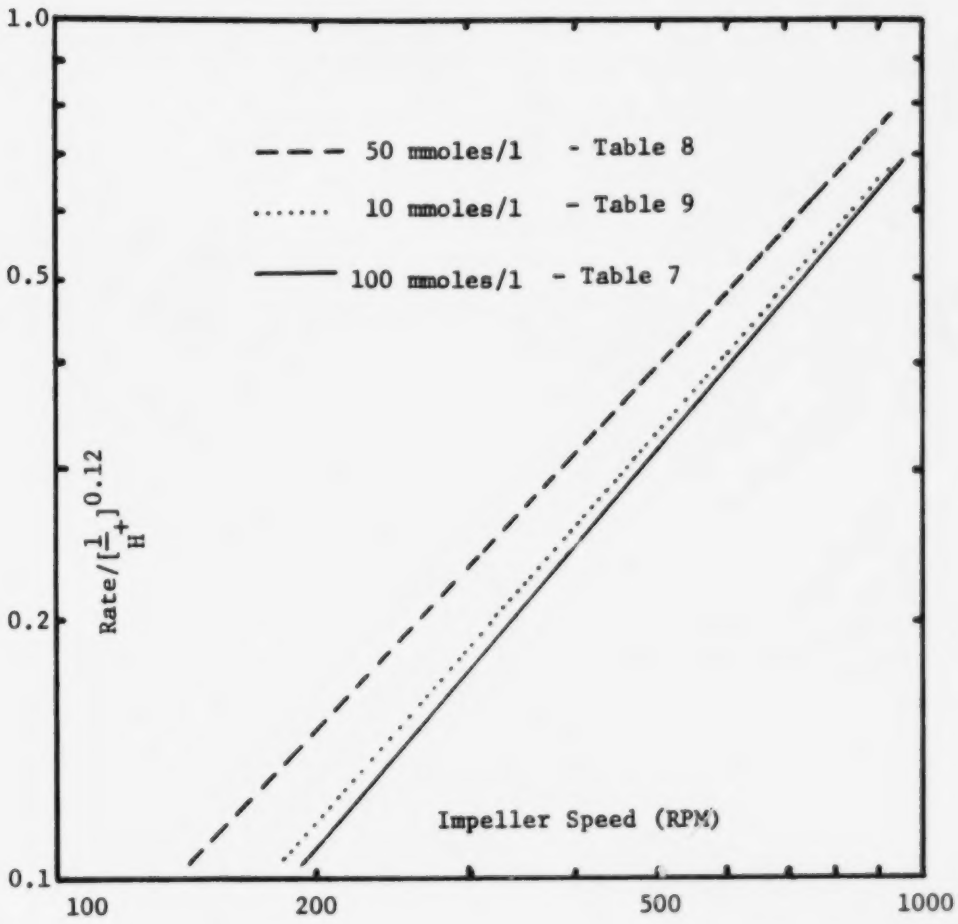

Figure V-4. Log Rate/$[\frac{1}{H^+}]^{0.12}$ vs. Log Impeller Rotation for Na_2SO_3 Feed at 4% Oxygen, Tables 7,8, and 9.

data was obtained by assuming the results were independent of sulfite ion concentration, although the data do not fall completely on one line.

Further data to study the effect of pH changes at a higher concentration of sulfite where the pH was again varied by the addition of sulfuric acid, appeared to be relatively independent of hydrogen ion concentration, i.e., a lower exponent was observed. This is again indicative of the complicated nature of the reaction showing that small changes in reaction conditions have subtle effects on the rate controlling steps.

Summary

It appears that results obtained in the CSTR are comparable with those obtained in the literature under similar conditions. Mass transfer effects are important over the range of conditions studied and oxygen concentration is the most important variable. Results are essentially independent of sulfite concentration, but proportional to pH (from pH 3 to pH 9) which could be interpreted as a dependence on hydroxyl ion concentration.

D. Experiments with Calcium Sulfite

A summary of the results with the calcium solutions and slurries is shown in Table V-4 with representative results of sodium sulfite for comparison. The first set of data was obtained on a saturated solution of calcium sulfite after solid had been allowed to settle. At pH of 7-8 the concentration of sulfite in solution is about 0.1 mmole per liter and the oxidation rate is very low--less than 0.1 micromoles per liter per second. At a pH of 3-4, the oxidation rate is higher by at least an order of magnitude. The concentration of sulfite in solution (i.e., bisulfite ion) is 15-20 mmoles per liter. A log-log plot of the data from Table 10 Appendix 2 is shown in Figure V-5. The oxidation rate was found to be proportional to total sulfite concentration (S_T) (effectively bisulfite with pH range of interest) and independent of pH according to the equation:

$$R_{ox} = 227 \times 10^{-6} [S_T]^{1.16}$$

The second set of data with a calcium sulfite slurry of about 0.2% gave oxidation rates of 1-2 micromoles/liter-sec. across the pH range 3-8, about equal to the rate for the saturated solution at low pH, but much higher than the saturation solution at high pH, showing that the solid is able to dissolve fast enough under these conditions to cause an increase in the overall oxidation rate.

The next group of experiments were carried out with calcium carbonate/calcium sulfite mixtures. With the saturated solutions at pH 7-8, the reaction rate appeared somewhat higher than for the sulfite alone, despite the lower solubility of sulfite in the mixture. However, these data are close to the limits of experimental determination. At the lower pH, the oxidation rate was

TABLE V-4 SUMMARY OF OXIDATION RATES FOR CALCIUM

Reactant	Oxidation rate ($\times 10^6$ moles/l-sec) pH 7-8	pH 3-4
$CaSO_3$ saturated solution	>0.1	1 - 2
$CaSO_3$ slurry (0.2%)	1 - 2	1 - 2
$CaCO_3/CaSO_3$ saturated solution	0.2-0.3	1 - 2
$CaCO_3/CaSO_3$ saturated solution + $CuSO_4$	0.3	-
$CaCO_3/CaSO_3$ saturated solution + Calnox	0.5	1
$CaCO_3/CaSO_3$ slurry (0.2%)	2	5
$CaCO_3/CaSO_3$ slurry (0.2%) + $CuSO_4$	2	5 - 6
Na_2SO_3solution (10 mmoles/l)	3 - 4	1 - 2 (H_2SO_4)* 3 - 4 (SO_2)*

* pH adjusted with H_2SO_4 and SO_2, respectively.

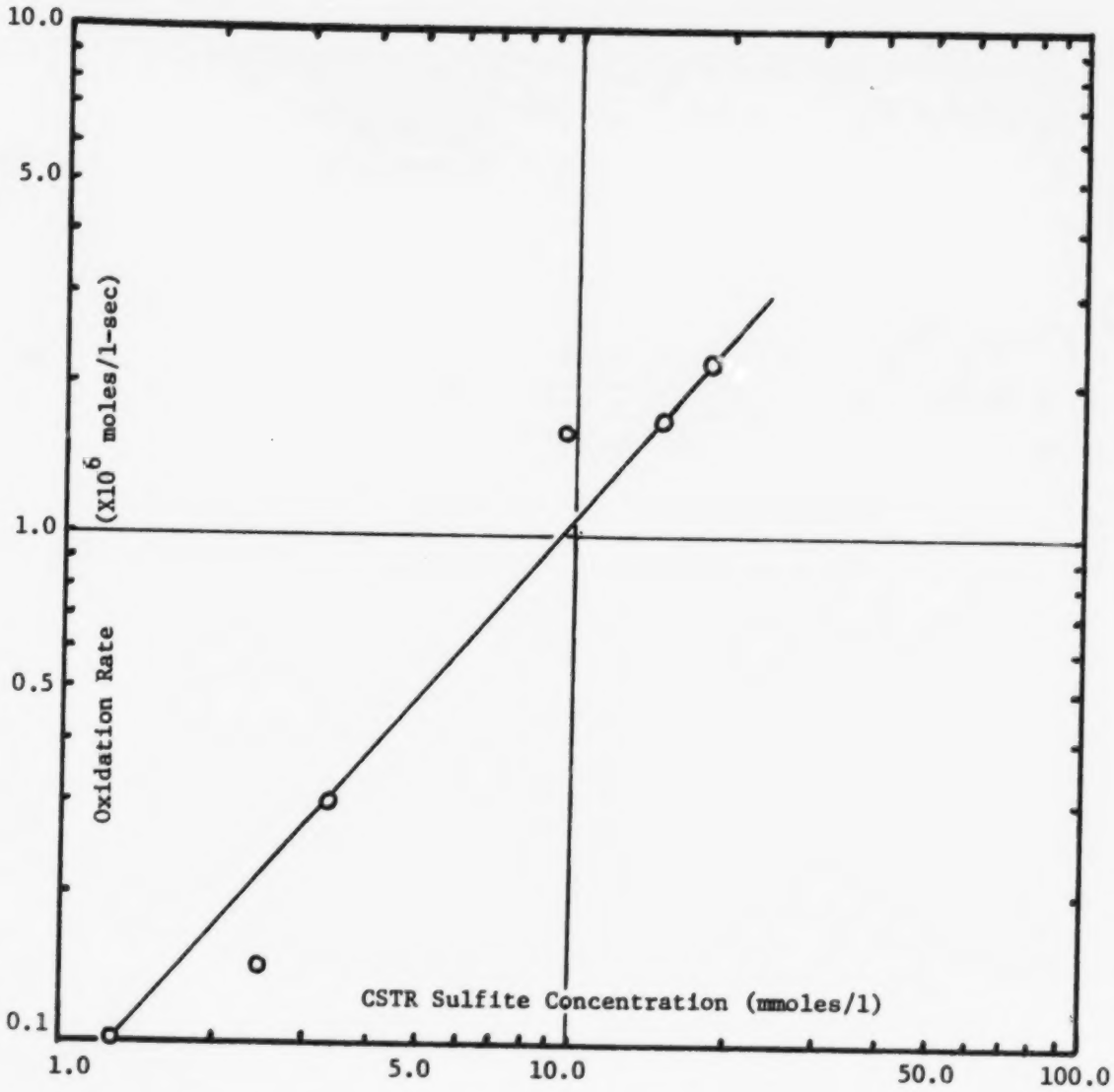

Figure V-5. Log Oxidation Rate vs. Log CSTR Sulfite Concentration for $CaSO_3$ Supernatant Feed (4% Oxygen, Impeller Speed = 625 RPM).

the same as for the saturated sulfite solution. The addition of $CuSO_4$ as a catalyst and the anti-scale agent, Calnox, in different tests did not appreciably alter the rates for mixed solutions. A slurry of calcium carbonate and calcium sulfite was used to determine the effect of solids dissolution in a mixed system. Rates were only slightly higher for sulfite slurry alone at pH 7-8, but significantly greater at pH 3-4. These latter values were the highest observed in all of the calcium sulfite systems; again, the addition of $CuSO_4$ did not greatly increase the oxidation rate in the mixed slurry.

It is noticeable that all the calcium solutions gave higher oxidation rates at the lower pH's. This is in direct contrast to the results for sodium sulfite also shown on Table V-4, where the oxidation rate was about 3-4 micromoles/liter-sec. at pH 7-8, higher than any of the calcium results observed at that level. On the acid side, the sodium data varied from about 1-4 micromoles/liter-sec., close to the same order as the results obtained for calcium solutions.

Summary

Saturated calcium sulfite solutions (no solid present) showed very low oxidation rates above pH 7, but reached rates an order of magnitude higher at pH 4. Oxidation rates were proportional to total sulfite concentration (effectively bisulfite ion concentration). Oxidation of calcium sulfite always resulted in a decrease in solution pH. The rate of oxidation of a 0.2% calcium sulfite slurry at pH 7 was much higher than the saturated solution and equivalent to that of a calcium sulfite saturated solution at pH 4. Thus, the rate of sulfite dissolution is a significant contributing factor to the rate of oxidation under normal operating conditions.

Saturated solutions of calcium carbonate/calcium sulfite oxidize at a slightly higher rate than calcium sulfite solution. Above pH 6, oxidation causes an increase in solution pH; below pH 6 oxidation causes a decrease in solution pH. It appears that above pH 6 there is sufficient carbonate present to neutralize the sulfate formed whereas below pH 6 sulfite is in excess.

Due to the dissolution effect noted earlier, mixed carbonate-sulfite slurries oxidize more rapidly than the corresponding solutions. Neither copper sulfate nor Calnox 214 DN appreciably affects oxidation rates. Since oxidation rate is strongly dependent on bisulfite ion concentration in calcium solutions, other cationic impurities such as sodium or magnesium, which can dramatically increase bisulfite concentration in solution in the range of pH 5-6, may have a strong effect on oxidation rate. Although the effect of oxygen partial pressure was not studied with calcium solutions, the effects noted with sodium sulfite suggest that the rate of oxidation might be higher in the hold tank than in the scrubbing tower due to the higher oxygen partial pressure over the hold tank.

REFERENCES FOR CHAPTER V

1. Reith, T., Physical Aspects of Bubble Dispersion in Liquids, Thesis, Delft Technical University (1968).

2. Astarita, G., Marucci, G., and Gioia, F., Proc. 3rd Europ. Symp. on Chemical Reaction Engineering, 195 Pergamon Press, London (1964).

3. de Waal, K.J.A., and Okeson, J.C., Chem. Eng. Sci. 21, 559 (1956).

4. Srivastava, R.D., McMillan, A.F., and Harris, J.J., Can. J. Chem. Eng. 46, 181 (1968).

5. Rand, M.C. and Gale, S.B. "Principles and Applications of Water Chemistry," Ed. Faust S.D. & Hunter, J.V., Wiley (1967) .

6. Cooper, C.M., Fernstrom, G.A., and Mille, S.A., Ind. Eng. Chem. 36, 504 (1944).

7. Fuller, E.C. & Crist, R. H., JACS 63, 1644 (1941).

8. Westerterp, K.R., Van Dierendonek & de Kraa, J.A., Chem. Eng. Sci. 18, 157 (1963).

VI. MATHEMATICAL MODEL OF PACKED BED SCRUBBER

A. Material Balances

A flow diagram of the bench scale scrubber system is shown in Figure VI-1. Since heat transfer in a packed column absorber is known to be very rapid, the system can be assumed to operate isothermally; that is, the variations in the liquid and gas temperatures throughout the system can be ignored for all practical purposes when the heat of reaction is negligibly small.

Overall Material Balances

The conservation of sulfur, carbon and calcium within the overall system shown in Figure VI-1 can be written as

Sulfur

$$M_{SO_2,0} + M_{SO_2,1} + M_{SO_2,2} + M[S]_M + MS_{S,M} - MS_{S,P} - M[S]_P = A_S \qquad \text{(VI-1)}$$

Carbon

$$M_{CO_2,0} + M_{CO_2,1} + M_{CO_2,2} + M[C]_M + MS_{C,M} - MS_{C,P} - M[C]_P = A_C \qquad \text{(VI-2)}$$

Calcium

$$MS_{Ca,M} + M[Ca]_M - MS_{Ca,P} - M[Ca]_p = A_{Ca} \qquad \text{(VI-3)}$$

Where $M_{SO_2,i}$ is the absorption rate of SO_2 in the $i^{\underline{th}}$ piece of equipment, (gmole/sec)

$M_{CO_2,i}$ is the absorption rate of CO_2 in the $i^{\underline{th}}$ piece of equipment, (gmole/sec),

$S_{k,l}$ is the total concentration of species k as solid in the $l^{\underline{th}}$ stream, (gmole/liter),

$[k]_l$ is the total liquid phase concentration of species k in the $l^{\underline{th}}$ stream, (gmole/liter),

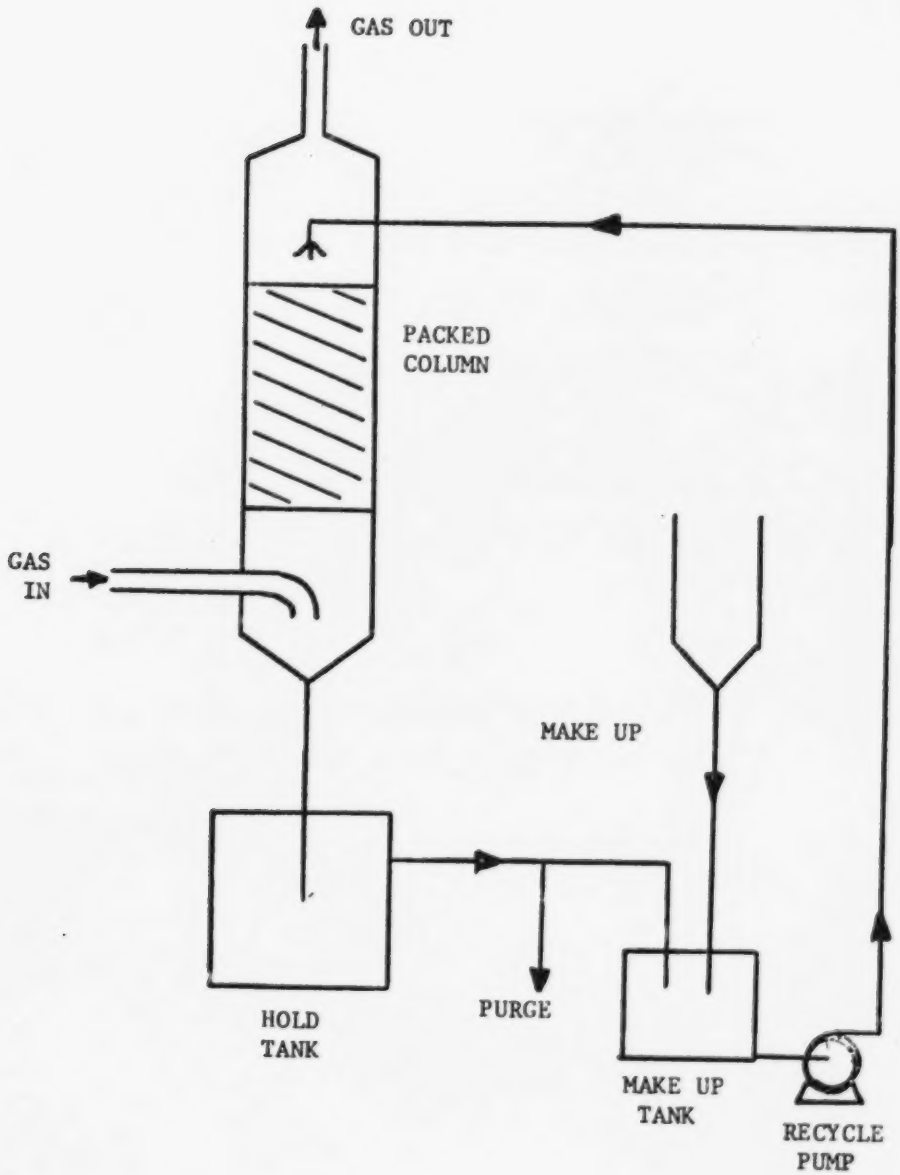

Figure VI-1. Line Diagram of Experimental Scrubbing Apparatus

A_k is the accumulation of species k as solid within the overall system, (gmole/sec),

and M is the make-up rate, (liter/sec).

When i = 0,1,2 the subscript refers to the scrubber, recharge tank and holding tank, respectively,

k = S,C,Ca the subscript refers to sulfur, carbon and calcium, respectively,

and l = M,P the subscript refers to the make-up and purge streams, respectively.

The above equations apply to steady state operation of the scrubber system (that is, steady state with respect to the liquid concentrations) and a constant rate of scale formation as indicated through the use of the accumulation terms (A_k).

Steady liquid concentrations may be inconsistent with the steady build-up of solids in the scrubber system. For example, it is known that the accumulation of scale in the scrubber causes an increase in the SO_2 removal which in turn would affect the liquid compositions. However, this process normally takes place slowly and it can be assumed that Equations VI-1 through VI-3 can be applied at each instant of time. This is equivalent to a quasi-steady state assumption.

Subtracting Equation VI-3 from the sum of Equations VI-1 and VI-2 gives

$$\sum_{i=0}^{2} (M_{SO_2,i} + M_{CO_2,i}) = M[\Delta_p - \Delta_M] \qquad \text{(VI-4)}$$

Where $\Delta_\ell = [S]_\ell + [C]_\ell - [Ca]_\ell$

Here the fact that the solid calcium salts have a one-to-one correspondence of calcium to sulfur or carbon has been used to eliminate the solid concentrations appearing in Equations VI-1 through VI-3. It can be noted that Equation VI-4 does not contain any solid compositions.

A further simplification of Equation VI-4 is possible if it is noted that $\Delta_M = 0$. This follows from the fact that the make-up slurry is formulated by mixing solid calcium salts of sulfur and/or carbon with water; then by stoichiometry $\Delta_M = 0$. Thus

$$\sum_{i=0}^{2} (M_{SO_2,i} + M_{CO_2,i}) = M\Delta_p \qquad \text{(VI-5)}$$

In the bench scale scrubber very little SO_2 evolution occurs in the hold or make-up tanks (except at very low pH). This is concluded for several reasons: (1) the tanks are for all practical purposes closed containers, (2) very little surface area is available for mass transfer between the liquid in the tank and the gas space above the liquid, and (3) if the partial pressure of SO_2 builds up to a significant level in the liquid phase, it will be preferentially discharged in the scrubber since in the scrubber conditions are conducive to mass transfer whereas in the hold or make-up tank they are not.

Under the assumption of no SO_2 evolution from the hold or make-up tank, Equation VI-5 becomes

$$M_{SO_2,0} + \sum_{i=0}^{2} M_{CO_2,i} = M\Delta_p \qquad \text{(VI-6)}$$

As defined above, the absorption rates $M_{SO_2,0}$ and $M_{CO_2,i}$ are positive for absorption. They are negative in sign when material is evolved from the system.

Without further assumptions Equation VI-6 does not appear to be useful. However, with the assumption that the liquid in the holding tank maintains equilibrium, the Delta concentration of the purge stream, Δ_p, and Equation

VI-6 take on unusual significance and utility as discussed below. (It is assumed that the slurry in the holding tank and the purge slurry has the same composition.)

Analysis of Holding Tank under the Equilibrium Assumption

The idea that the liquid in the holding tank maintains equilibrium has been used by Wen and Uchida[8] to successfully analyze recycle scrubber systems using limestone slurry and stirred holding tanks with residence times between 10 and 40 minutes. The minimum time in which equilibrium in a stirred tank is reached for limestone slurry systems is not well known. Borgwardt[3] reported a kinetic expression which could predict the volumetric rate of sulfite disappearance from limestone scrubbing slurry fairly accurately for stirred tank reactors indicating 4 to 6 minutes minimum residence time are required for the solution to reach equilibrium.

Under the assumption of equilibrium of the holding tank, the delta concentration, Δ_p, can be related to the liquid phase concentrations of the other species present through equilibrium calculations. Figure VI-2 presents a typical equilibrium graph of pH versus concentration. However, the reverse is not true. It can be seen from Figure VI-2 that at certain delta concentrations two or three pH's are possible. Thus if Δ_p is calculated from Equation VI-6, some mechanism must be provided to resolve the pH ambiguity which might occur. This can be done by following the relationships between pH and the amount of SO_2 absorbed and CO_2 evolved from the system through the use of a "titration" diagram.

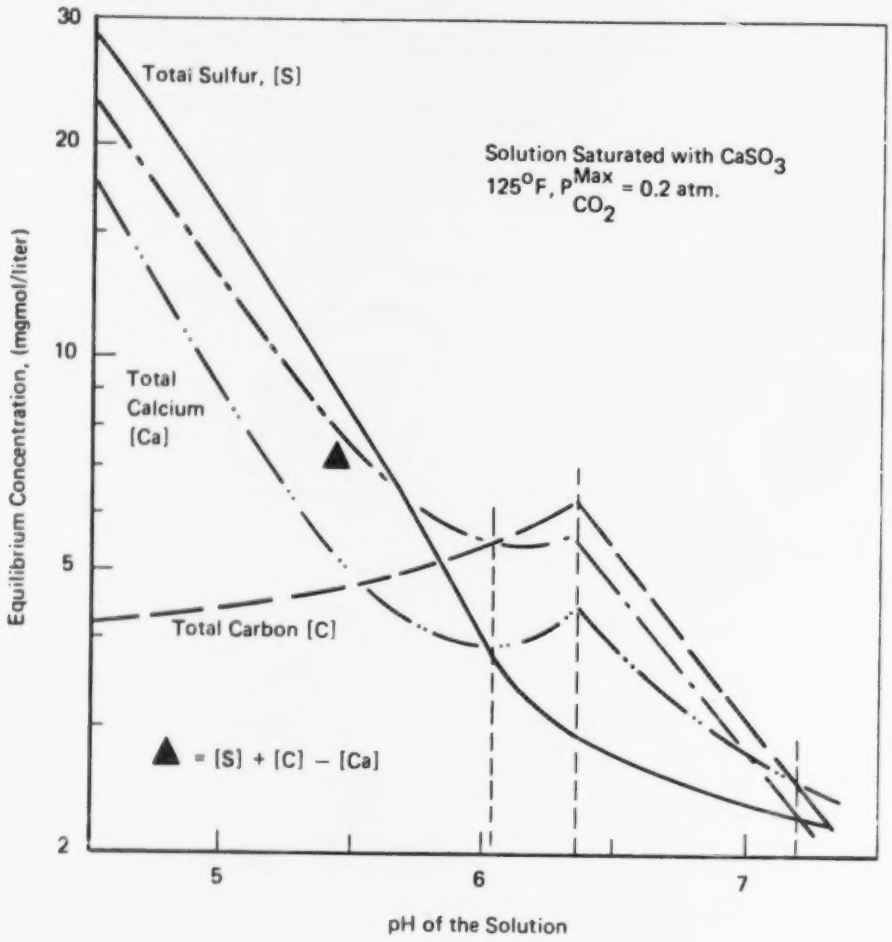

FIGURE VI–2 EQUILIBRIUM CONCENTRATIONS OF TOTAL SULFUR, CARBON AND CALCIUM AND THE DELTA CONCENTRATION AS A FUNCTION OF pH. SOLUTION SATURATED WITH $CaSO_3$, TEMPERATURE IS 125^oF AND PARTIAL PRESSURE OF CO_2 RESTRICTED TO LESS THAN 0.2 ATM.

"Titration" Diagrams

The scrubbing operation can be viewed as a process in which a volume of make-up slurry is allowed to absorb a certain number of moles of SO_2 and CO_2 is allowed to evolve from the volume of make-up slurry. The CO_2 is evolved in accordance with the following rules.

1. No CO_2 evolution occurs until the partial pressure of CO_2 in equilibrium with the make-up slurry to which SO_2 has been added reaches a certain maximum partial pressure of CO_2, $P_{CO_2}^{MAX}$.
2. Once the partial pressure of CO_2 reaches $P_{CO_2}^{MAX}$, only enough CO_2 is evolved from the solution so as to maintain the partial pressure above the solution at $P_{CO_2}^{MAX}$.

The process described above is similar to an ordinary titration experiment. The progress of the titration can be followed on a titration diagram which can be prepared using equilibrium curves such as the one shown in Figure VI-2 and Equation VI-6 rearranged in the following form.

$$\Delta_p = \frac{M_{SO_2,0}}{M} + \sum_{i=0}^{2} \frac{M_{CO_2,i}}{M} \qquad \text{(VI-7)}$$

The terms on the right hand side of this equation represent the moles of SO_2 and CO_2 added to the system per volume of make-up slurry, respectively.

In what is to follow, the construction of the titration diagram for the following conditions will be described:

1) Make-up slurry is 0.5 weight per cent $CaCO_3$.
2) The liquid temperature is 125°F.
3) The limiting partial pressure of CO_2, $P_{CO_2}^{MAX}$, is 0.2 atm.

4) Only $CaCO_3$ and $CaSO_3$ can be present in solid form.

and 5) Sulfate ions are not present.

Figure VI-2 is the equilibrium diagram which is applicable at these conditions. In this figure solid $CaSO_3$ is present at every pH and $CaCO_3$ is present as solid above a pH of 6.4 and abeent below this pH. The pH of 6.4 corresponds to the point at which the partial pressure of CO_2 reaches $P_{CO_2}^{MAX}$ and is referred to as the invariant point. At pH's below the invariant pH the partial pressure of CO_2 is maintained at $P_{CO_2}^{MAX}$ in accordance with the CO_2 evolution rules established above.

At the start of the titration only $CaCO_3$ is present in the slurry so the initial pH cannot be found on Figure VI-2; however, this pH does not have to be known precisely since in all our experiments enough SO_2 is added to the slurry so that the final chemical composition of the slurry is far removed from this point. As SO_2 is added to the slurry the pH will fall and at the pH of 7.6 the calcium in solution will equal the total carbon in solution. It is at this point that $CaSO_3$ begins to precipitate from solution. This point also is the end of Region I and the beginning of Region II as shown in the titration graph in Figure VI-3.

In Region I the amount of SO_2 absorbed per liter of make-up is equal to the liquid phase concentration of total sulfur, [S]. Thus over this region the pH of the slurry as a function SO_2 absorbed per liter of slurry can be followed easily using the equilibrium diagram (Figure VI-2).

Region II of the titration (as shown in Figure VI-3) extends from the point where $CaSO_3$ first precipitates out of solution to the invariant point.

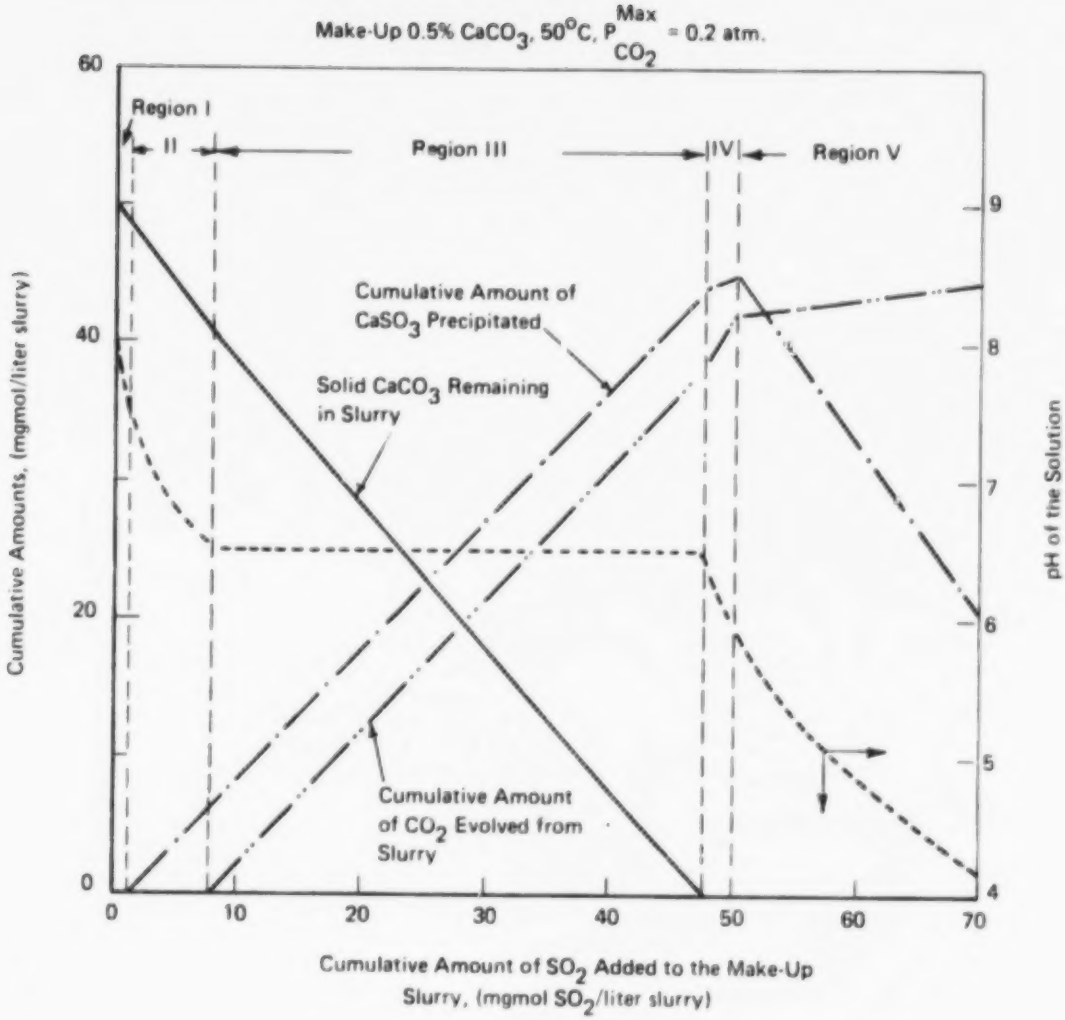

FIGURE VI–3 TITRATION DIAGRAM FOR THE $CaCO_3$–SO_2 SYSTEM

Since the pH range of Region II lies above the invariant pH, CO_2 does not evolve from the solution in this region as discussed previously. Thus in Region II the liquid phase concentration of total carbon, [C], is an accurate measure of the $CaSO_3$ precipitated. The pH at any point in Region II can be calculated from the total amount of SO_2 added per liter of make-up slurry using Equation VI-7. Thus the other concentrations necessary to calculate the amount of $CaCO_3$ dissolved or $CaCO_3$ precipitated as described above can be obtained from the equilibrium diagram.

Region III in the titration is the invariant region. This region starts at the point at which the partial pressure of CO_2 reaches $P_{CO_2}^{MAX}$. It is characteristic of this region that all the solid $CaCO_3$ must finish dissolving before the system leaves this pH and this region and the liquid concentrations remain constant here. Thus by Equation VI-7 the moles of SO_2 absorbed in this region must be equal to the moles of CO_2 evolved and the moles of $CaCO_3$ dissolved must equal the moles of $CaSO_3$ precipitated in the invariant region. Region III appears in Figure VI-3 as the region of constant pH.

Region IV of the titration lies between the invariant pH and the pH at which the minimum in the total calcium curve occurs. In this region no solid $CaCO_3$ is present and the amount of SO_2 added per liter of slurry in this region equals the increase in the total sulfur, [S], in solution plus the decrease in the total calcium [Ca] in solution.

Region V is the region which has a pH less than the pH at which the minimum in the total calcium curve occurs. In this region solid $CaSO_3$ dissolves as more SO_2 is added to the slurry and the added SO_2 per liter of slurry equals the increase in the total sulfur concentration minus the increase in total calcium in solution.

The overall titration diagram is shown in Figure VI-3. Here the pH and accumulative amounts of CO_2 evolved, $CaCO_3$ dissolved and $CaSO_3$ precipitated are shown as a function of the accumulative amounts of SO_2 added per liter of make-up slurry.

The most important curve on the titration diagrams for the purpose of simulating the ADL scrubber system is the pH versus SO_2 absorbed curve. This curve can be used in conjunction with the pH-SO_2 absorption relationship which characterizes the packed bed scrubber. This latter relationship is discussed in Section B. The pH and SO_2 absorption at which both the titration and scrubber characteristics are satisfied is the operating point of the scrubber recycle system. This will be discussed in more detail in Section C.

The calcium utilization for the scrubber-recycle system can be calculated from the titration diagram as long as there is no accumulation of $CaCO_3$ in the system. Suppose, for example, that the titration and scrubber characteristics are both satisfied at 40 mgmol per liter slurry. Since the initial amount of $CaCO_3$ was 50 mgmol per liter of make-up slurry, the calcium utilization is 84%.

B. Absorption Parameters

In the analysis and modeling of scrubber systems probably the most important quantities which must be known are the physical mass transfer coefficients for the scrubber.

Correlations for both the liquid and gas side physical mass transfer coefficients in packed beds are plentiful in the literature[1,5,6] and can predict these quantities fairly accurately if wall and end effects are negligible. For small diameter packed beds such as the one used here, where wall and end effects are apparently significant, corrections must be made in these mass transfer coefficient correlations.

Although the mechanism of SO_2 absorption into limestone slurry is not fully understood and the number of reactions which occur upon SO_2 absorption are too numerous to develop a complete analytical treatment of SO_2 absorption into a limestone slurry; SO_2 absorption can, for the present time, be handled empirically through an enhancement factor.

In this section the correlations for the mass transfer coefficients for physical absorption and enhancement factor for the A. D. Little scrubber will be discussed.

Mass Transfer Coefficients for Physical Absorption

SO_2 absorption experiments[2] using NaOH solution as the scrubbing liquor has been carried out in the A. D. Little packed column. At the values of pH ($8.9<pH<12.8$) which prevailed in these experiments, the partial pressure of SO_2 in equilibrium with the scrubbing liquor is nil; and therefore, the transfer of SO_2 to the NaOH solution can be considered, for all practical purposes, gas film controlled.

Under the assumption of gas film controlled absorption of SO_2, the governing equation for the transfer of SO_2 in the scrubber is

$$\frac{-\hat{G}}{P_T}\frac{dP_{SO_2}}{d_z} = (k_g a)P_{SO_2} \qquad \text{(VI-8)}$$

Where $\hat{G}$ is the molar gas flow rate, (gmole/cm^{2}sec),

P_{SO_2} is the partial pressure of SO_2 in the bulk gas phase, (atm),

P_T is the total pressure, (atm),

z is the height of the column measured from the bottom, (cm),

k_g is the gas side mass transfer coefficient for physical absorption, (gmole/cm^2 atm sec),

and a is the specific interfacial area available to mass transfer, (cm^{-1}).

Integration of Equation VI-8 over the height of the packed column yields

$$k_g a = \frac{\hat{G}}{P_T Z} \ln \frac{P_{SO_2}^{in}}{P_{SO_2}^{out}} \qquad \text{(VI-9)}$$

Where Z is the total height of the packed column, (cm),

and $P_{SO_2}^{in}$, $P_{SO_2}^{out}$ are the inlet and outlet partial pressure of SO_2, (atm).

The gas side mass transfer coefficient for physical absorption, $k_g a$, for ADL's packed column can be calculated using Equation VI-9 and the experimental data for SO_2 scrubbing with NaOH solutions[2]. The calculated coefficients are shown in Table VI-1.

TABLE VI-1

Gas Side Mass Transfer Coefficients
for Physical Absorption for A.D. Little's Packed Column

Run #	$\hat{G}$ $\frac{gmole}{cm^2 sec}$	$\hat{L}$ $\frac{g}{cm^2 sec}$	$k_g a$ $\frac{gmole}{cm^3 atm.sec}$
3	1.98×10^{-3}	0.312	2.39×10^{-4}
4	1.92×10^{-3}	0.203	2.07×10^{-4}
5	2.60×10^{-3}	0.203	1.96×10^{-4}

With reference to Table VI-1, Run Nos. 1, 2 and 6 have been excluded. For Run Nos. 1 and 2, the percent of SO_2 removal was reported to be greater than 97.5. The exact percent removal must be known at these high removal percentages because the calculated $k_g a$ is extremely sensitive to the SO_2 removal in this range. Run No. 6 was discarded because it appeared inconsistant with the remainder of the runs.

Not enough SO_2-NaOH scrubbing data have been analyzed to establish the functional dependence of the gas side mass transfer coefficient on flow rates. However, if the functional dependence of $k_g a$ on the gas and liquid flow rates, which is reported in the literature[1], is assumed to be valid for the $k_g a$ in A. D. Little's packed column, then a relationship between the gas side mass transfer coefficient for physical absorption and the liquid and gas flow rates can be established.

The correlation for the gas side mass transfer coefficients for a column packed with 1/2" Berl saddles operating under gas and liquid flow rate similar to the flow rates used in the experiments is given by:[1]

$$k_g a = \alpha \hat{L}^{0.24} \hat{G}^{0.7} \qquad \text{(VI-10)}$$

Where $\alpha = 0.00792$

If the same functional form of $k_g a$ is assumed for the A. D. Little data shown in Table VI-1, the value of α which minimizes the sum of the squares of the difference between the calculated and experimental gas side mass transfer coefficients for the packed column is

$$\alpha_{ADL} = 0.0222$$

The correlation of the gas side mass transfer coefficient for physical absorption is then

$$k_g a = 0.0222 \hat{L}^{0.24} \hat{G}^{0.7} \qquad \text{(VI-11)}$$

The value of α for the A. D. Little packed column is larger than the α value reported in the literature. This is due in part to the fact that Equation VI-10 is a correlation for Berl saddles whereas Equation VI-11 applies to Intalox saddles which have a larger specific interfacial area than Berl saddles. Also the increase in α may be due to an increase in interfacial area resulting from end and wall effects in the scrubber.

By assuming the liquid side mass transfer coefficient for physical absorption in the scrubber has the same functional dependence on flow rates as Sherwood's[1] correlation for liquid film coefficients in beds packed with Berl saddles, a correlation for $k_L a$ in terms of the liquid flow rate can be developed.

Sherwood's correlation for 1/2" Berl saddles is

$$k_L a = \beta \hat{L}^{0.72} \qquad \text{(VI-12)}$$

Where k_L is the liquid side mass transfer coefficient for physical absorption, (cm/sec)

and $\beta = 0.0270$

If the constant β is affected by the interfacial surface area in similar manner as the value of α in the $k_g a$ correlations then the correlations for $k_L a$ (liquid side mass transfer coefficient for physical absorption) in the A. D. Little packed column is

$$k_L a = \beta \left(\frac{\alpha ADL}{\alpha}\right) \hat{L}^{0.72} = 0.0758 \hat{L}^{0.72} \qquad \text{(VI-13)}$$

Mass Transfer with Chemical Reaction in the Liquid Phase

The molar flux of SO_2 across the gas-liquid interface in a wet scrubber can be written in terms of the gas or liquid side resistance as

$$N_{SO_2} = k_g (P_{SO_2} - P^i_{SO_2}) = k_L \phi (C_{A_i} - C_A) \qquad \text{(VI-14)}$$

Where N_{SO_2} is moles of SO_2 absorbed per unit time per unit interfacial area, (mole/cm^{2}sec),

$P^i_{SO_2}$ is the partial pressure of SO_2 at the gas-liquid interface, (atm),

ϕ is the enhancement factor for mass transfer in the liquid film due to chemical reaction, (dimensionless),

C_{A_i} is the H_2SO_3 concentration at the gas-liquid interface, (gmole/cm^3),

and C_A is the H_2SO_3 concentration in the bulk liquid phase, (gmol/cm^3).

The enhancement factor, ϕ, takes into account the reaction of the diffusing H_2SO_3 with components found in the liquid phase.

The concentration of H_2SO_3 at the gas-liquid interface, C_{A_i}, can be related to the partial pressure of SO_2 at the interface, $P^i_{SO_2}$, by Henry's law

$$P^i_{SO_2} = HC_{A_i} \qquad \text{(VI-15)}$$

Where H is the Henry's law constant, (atm cm^3/gmol).

This equation holds for sufficiently dilute solutions.

The Henry's law constant, H, as a function of temperature has been given by Vivian[7] as

$$\ln H = 17.360 - \frac{3175.2}{T} \qquad \text{(VI-16)}$$

Where T is the liquid temperature in degrees Kelvin.

An expression for the interfacial concentration of H_2SO_3, C_{A_i}, can be obtained by substituting Equation VI-15 into VI-14.

$$P^i_{SO_2} = \frac{k_g P_{SO_2} + \frac{k_L \phi}{H} P^*_{SO_2}}{k_g + \frac{k_L \phi}{H}} \qquad \text{(VI-17)}$$

Where $P^*_{SO_2}$ is the partial pressure of SO_2 which could be maintained in equilibrium with the bulk liquid phase, (atm).

Substitution of this equation in Equation VI-14 gives

$$N_{SO_2} = \left[\frac{1}{k_g} + \frac{H}{k_L \phi}\right]^i (P_{SO_2} - P^*_{SO_2}) \qquad \text{(VI-18)}$$

The rate of SO_2 absorption in a differential height of the scrubber, dz, can be written as

$$\frac{-\hat{G}}{P_T}\frac{dP_{SO_2}}{dz} = \left[\frac{1}{k_g a} + \frac{H}{\phi k_L a}\right]^{-1} (P_{SO_2} - P^*_{SO_2}) \qquad \text{(VI-19)}$$

In Equation VI-19 both ϕ and $P^*_{SO_2}$ are functions of position in the column and both depend on the mechanism of SO_2 adsorption into recycle limestone slurries. For convenience, the enhancement actor can be defined such that Equation VI-19 can be written with $P^*_{SO_2}$. Thus

$$\frac{-\hat{G}}{P_T}\frac{dP_{SO_2}}{dz} = \left[\frac{1}{k_g a} + \frac{H}{\phi k_L a}\right]^{-1} P_{SO_2} \qquad \text{(VI-20)}$$

It must be noted that this equation is approximately correct and no assumption about ϕ is necessary if the liquid pH is above 4.7. Above this pH $P_{SO_2} >> P^*_{SO_2}$ and $P^*_{SO_2}$ can be ignored relative to P_{SO_2}, the partial pressure of SO_2 in the bulk gas phase.

Equation VI-20 can be integrated over the height of the packed column to give

$$\frac{\hat{G}}{P_T} \ln \frac{P^{in}_{SO_2}}{P^{out}_{SO_2}} = \int_o^Z \left[\frac{1}{k_g a} + \frac{H}{\phi k_L a}\right]^{-1} dz = \int_o^Z K_G a \, dz \qquad \text{(VI-21)}$$

Where $K_G a = \left[\frac{1}{k_g a} + \frac{H}{\phi k_L a}\right]^{-1}$ and is called the overall gas side mass transfer coefficient, (gmol/cm^{3}atm.sec).

Applying the mean value theorem to Equation VI-21 yields

$$\frac{\hat{G}}{ZP_T} \ln \frac{P^{in}_{SO_2}}{P^{out}_{SO_2}} = \overline{K_G a} = \left[\frac{1}{k_g a} + \frac{H}{\bar{\phi} k_L a}\right]^{-1} \qquad \text{(VI-22)}$$

Where $\bar{\phi}$ and $\overline{K_G a}$ are the "average" enhancement factor and the "average" overall mass transfer coefficient, respectfully.

Arthur D Little Inc

The "average" enhancement factor, $\bar{\phi}$ was calculated from Equation VI-22 and our experiment data[2]. As can be seen in Figure (VI-4), the enhancement factor is a strong function of pH. The enhancement factor was found to be nearly independent of the liquid recycle rate and temperature.

Large values of the enhancement factor correspond to the gas film being the dominating resistance to the transfer of SO_2 and similarly small values of the enhancement factor indicate the liquid film resistance to be important.

If Equation VI-9 were used to calculate $k_g a$ for the $CaCO_3$ data, i.e., assuming zero interfacial partial pressure of SO_2, the calculated $k_g a$ would be a strong function of pH because the liquid film resistances had been ignored. However, the true gas film mass transfer coefficient must be greater than the $k_g a$ value calculated from Equation (VI-9) using the $CaCO_3$ data. The maximum $k_g a$ calculated using Equation (VI-9) is 37.4 and occurs at pH of about 6.75. The $k_g a$ predicted by Equation (VI-11) for the same flow rates of gas and liquid is 37.8. This agreement is very good and tends to validate the assumptions made in obtaining the correlation for the gas side mass transfer coefficient (Equation (VI-11)) from the NaOH scrubbing data for the packed bed unit.

The correlations for the gas and liquid film mass transfer coefficients for physical absorption in the packed bed given by Equations (VI-11) and (VI-13), respectively, along with the empirical correlation for the enhancement factor, $\bar{\phi}$, given in Figure VI-4 can be used for predicting SO_2 removals in the A. D. Little scrubber. However, the value of the enhancement factor, should only be used within the limits of the data from which it was obtained (Table VI-2).

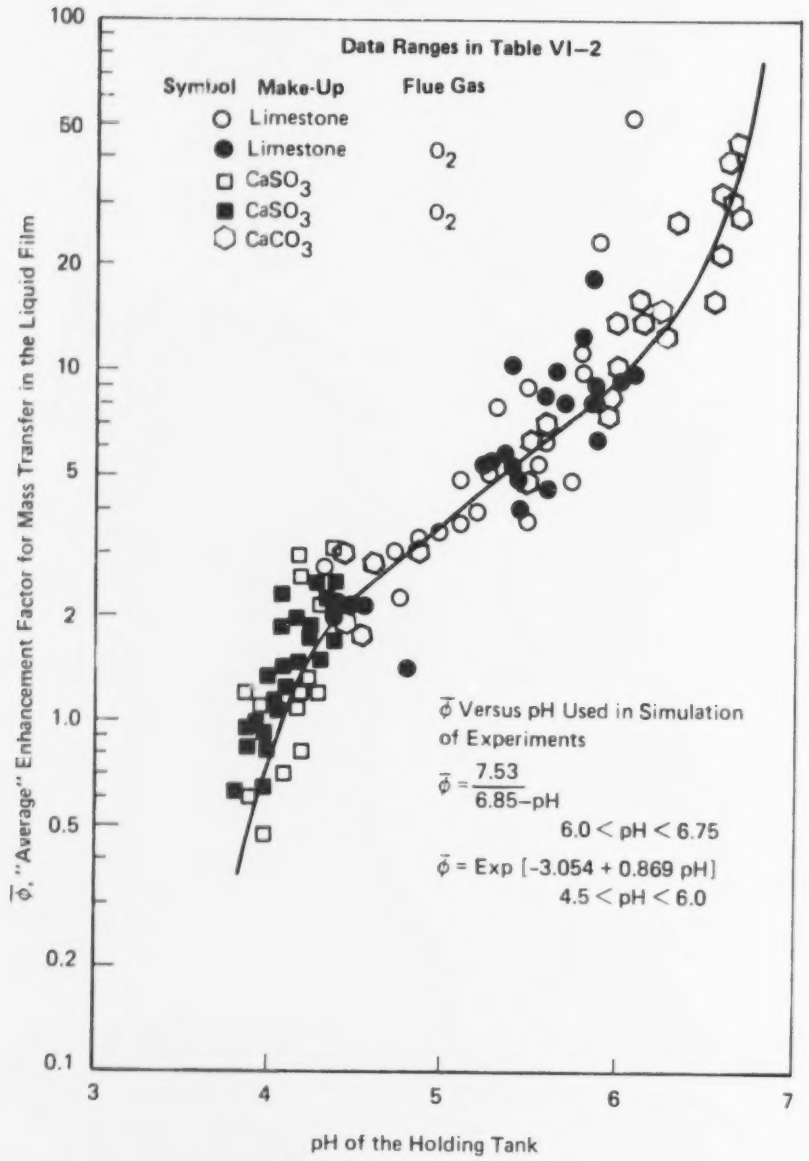

FIGURE VI–4 THE "AVERAGE" ENHANCEMENT FACTOR FOR MASS TRANSFER IN THE LIQUID FILM IN PACKED BED AS A FUNCTION OF THE pH OF THE HOLDING TANK IN SCRUBBER RECYCLE SYSTEM

TABLE VI-2

Range of Data Used in the Construction of Figure VI-4

	Scrubbing Slurry		
	0.5≤$CaCO_3$≤1.0	0.5≤Shawnee≤Limestone 0.6	0.5% $CaSO_3$
Make-up Rate (gpm)	1.3 to 5.2	1.3 to 5.4	1.7 to 6.8
Recycle Rate (gpm)	0.25, 0.50, 1.0	0.25, 0.5, 1.0	0.25, 0.5, 1.0
Gas Flow Rate (scfm)	5	5.0, 5.2	4.8 to 5.2
% O_2 in Gas	0%	0%, 4%	0%, 4%
Inlet SO_2 (ppm)	2000	2000,2300	2300
Liquid Temperature (°F)	100, 125	100, 125	100, 125
Stoichiometry	0.4 to 2.8	0.3 to 1.70	---------

A comparison between the calculated and experimental SO_2 removals is shown in Figure VI-5. Here the percent of SO_2 removal was calculated using Equation (VI-22) and the value of the enhancement factor given by the solid line in Figure VI-4. The experimentally observed pH was used to evaluate the enhancement factor in Figure VI-4. It can be seen from Figure VI-5 that most of the data for SO_2 removals for Shawnee limestone and $CaCO_3$ are within the ten percent error band; however, the $CaSO_3$ data for SO_2 removals are quite scattered and is due to the scatter of the enhancement factor data and error in drawing the line through the enhancement factor data in Figure VI-4.

C. Simulation of the A. D. Little Scrubber System

In Section A the titration diagram, which relates the amount of SO_2 absorbed in the scrubber per volume of make-up slurry to the pH of the holding tank, was described.

In Section B the relationship between the amount of SO_2 absorbed in the scrubber, the gas and liquid flow rates through the scrubber, and the pH of the holding tank was given by Equation (VI-22) as

$$\frac{\dot{G}}{ZP_T} \ln \frac{P^{in}_{SO_2}}{P^{out}_{SO_2}} = \overline{K_G a} \qquad \text{(VI-22)}$$

The amount of SO_2 absorbed in the scrubber per liter of make-up slurry is given by

$$\frac{M_{SO_2,O}}{M} = \frac{GS}{MP_T} (P^{in}_{SO_2} - P^{out}_{SO_2}) \qquad \text{(VI-23)}$$

Where S is the gross sectional area of the packed column, (cm^2)

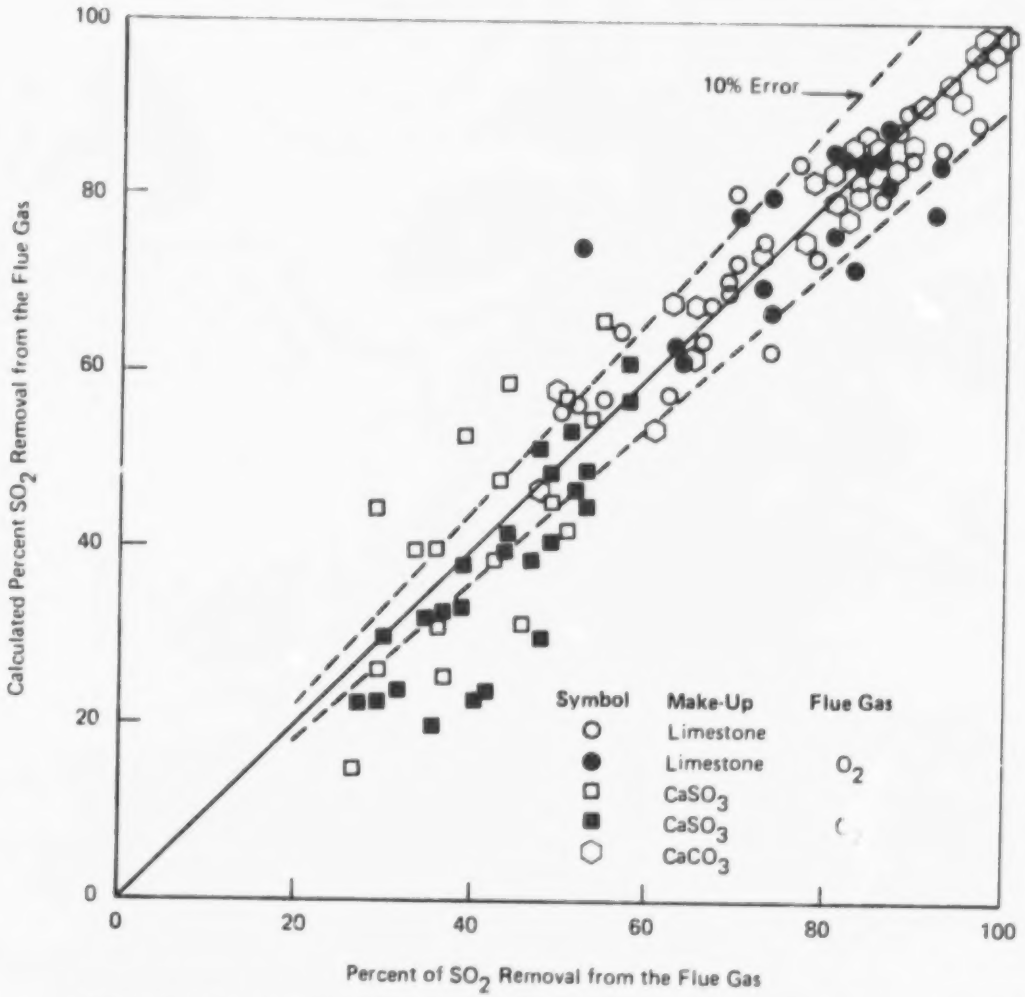

FIGURE VI–5 COMPARISON OF THE PERCENT SO_2 REMOVAL FROM THE FLUE GAS WITH THE PREDICTED PERCENT SO_2 REMOVAL CALCULATED USING THE OBSERVED pH OF THE HOLDING TANK TO EVALUATE THE ENHANCEMENT FACTOR

Substitution of Equation VI-22 into this equation gives

$$\frac{M_{SO_2,O}}{M} = \frac{GS}{MP_T} P^{in}_{SO_2} \left[1-\exp\left(-\frac{\overline{K_G a}\ ZP_T}{\hat{G}}\right)\right] \qquad \text{(VI-24)}$$

Once the flow rates, total pressure and the inlet partial pressure of SO_2 are fixed, the right hand side of Equation VI-24 becomes only a function of the pH of the holding tank. Equation VI-24 can be thought of as an equation describing the scrubber characteristics in terms of the pH of the liquor and the amount of SO_2 absorbed in the packed bed.

Two relationships between the amount of SO_2 absorbed in the column per volume of make-up slurry and the pH of the holding tank have been established. One is given by the titration diagram as shown in Figure VI-3 and the other is the scrubber characteristic which is given by Equation VI-24. At an operating point of the scrubber-recycle system both of these relationships must be satisfied.

In Figure VI-6 the titration diagram for $P^{MAX}_{CO_2}$ = 0.2 and 1.0 atm., and the scrubber characteristic for several make-up rates and a recycle rate of 0.5 gal/min. have been superimposed. The intersection of the titration line and the scrubber characteristic can be interpreted as an operating point of the scrubber-recycle system.

The procedure described above for finding the operating point of the scrubber-reyclce system has been used to simulate various experiments carried out by A. D. Little. In these simulations the maximum partial pressure of CO_2 was taken to be 0.2 atm. This value of the maximum partial pressure of CO_2 gave the best agreement between the observed and

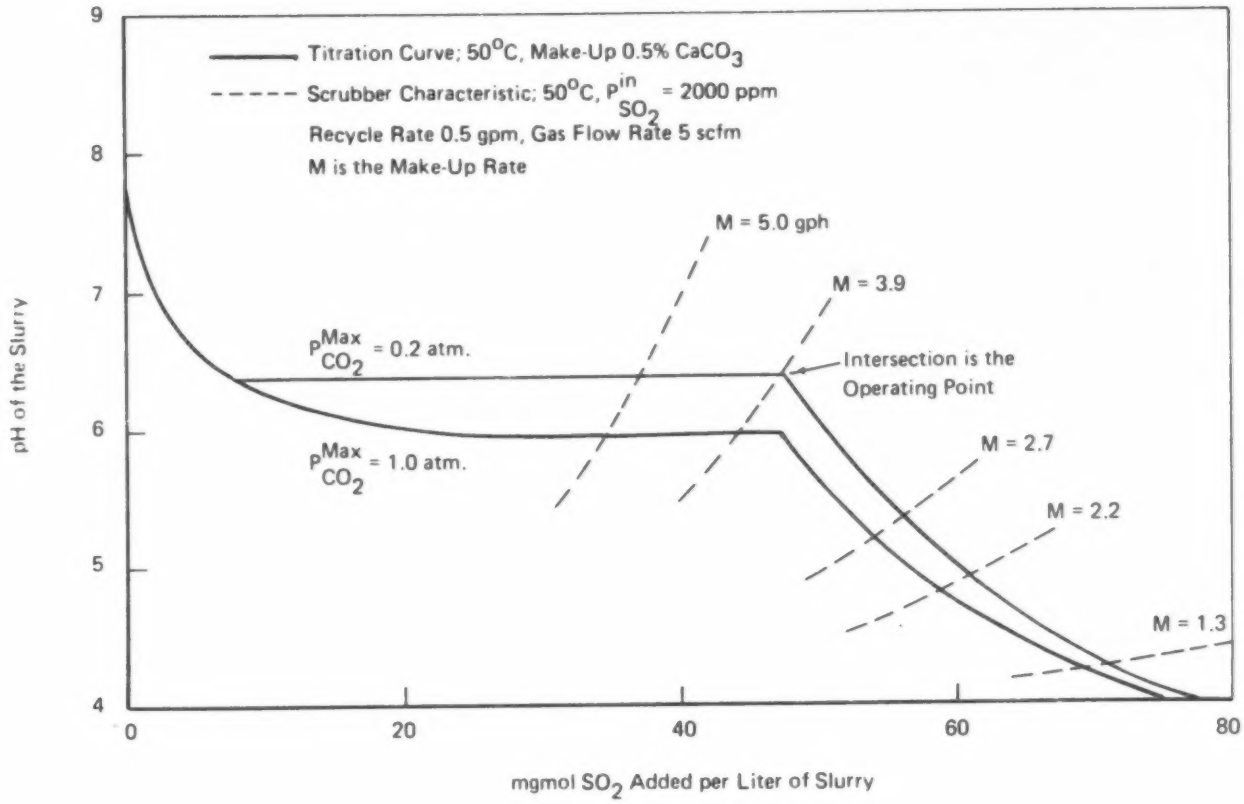

FIGURE VI–6 GRAPHICAL DETERMINATION OF THE OPERATING POINT OF THE SCRUBBER–RECYCLE SYSTEM

calculated pH of the holding tank. This agreement is shown in Figure VI-7 and it can be seen that in the majority of cases the observed and calculated pH's are within one-half of a pH unit of each other.

The choice of the maximum partial pressure of CO_2 equal to 0.2 results in the calculated percent SO_2 removal being slightly less than the observed percent SO_2 removal. However, as can be seen in Figure VI-8, the agreement between these two quantities is still fairly good. The agreement could be made better by choosing a slightly higher value for the maximum partial pressure of CO_2; however, this would increase the error between the observed and calculated pH of the holding tank. The fact that the CO_2 partial pressure in the holding could vary sometimes considerably, $P_{CO_2}^{MAX} = 0.2$ atm. on the average, seems reasonable.

Also, agreement could possibly be improved between the observed and calculated pH of the holding tank and percent SO_2 removal if a more accurate value of total calcium concentration (liquid plus solid) in the make-up slurry had been used in the simulations. For example, in Run 22 it was reported that the make-up consisted of a 0.5 percent (by weight) $CaCO_3$ in the slurry and this was the value used in the simulations. However, chemical analysis of the make-up slurry revealed that the total calcium concentration of 50 mgmol/liter. It is not known why this anomaly occured; however, the total calcium concentration in the make-up feed is very important in constructing the titration curve and should be known accurately.

Sulfite oxidation in the scrubber-recycle system does not appear to pose any particular problem in simulating the system by the method described above. Figure VI-9 shows the pH titration curves for a make-up slurry of

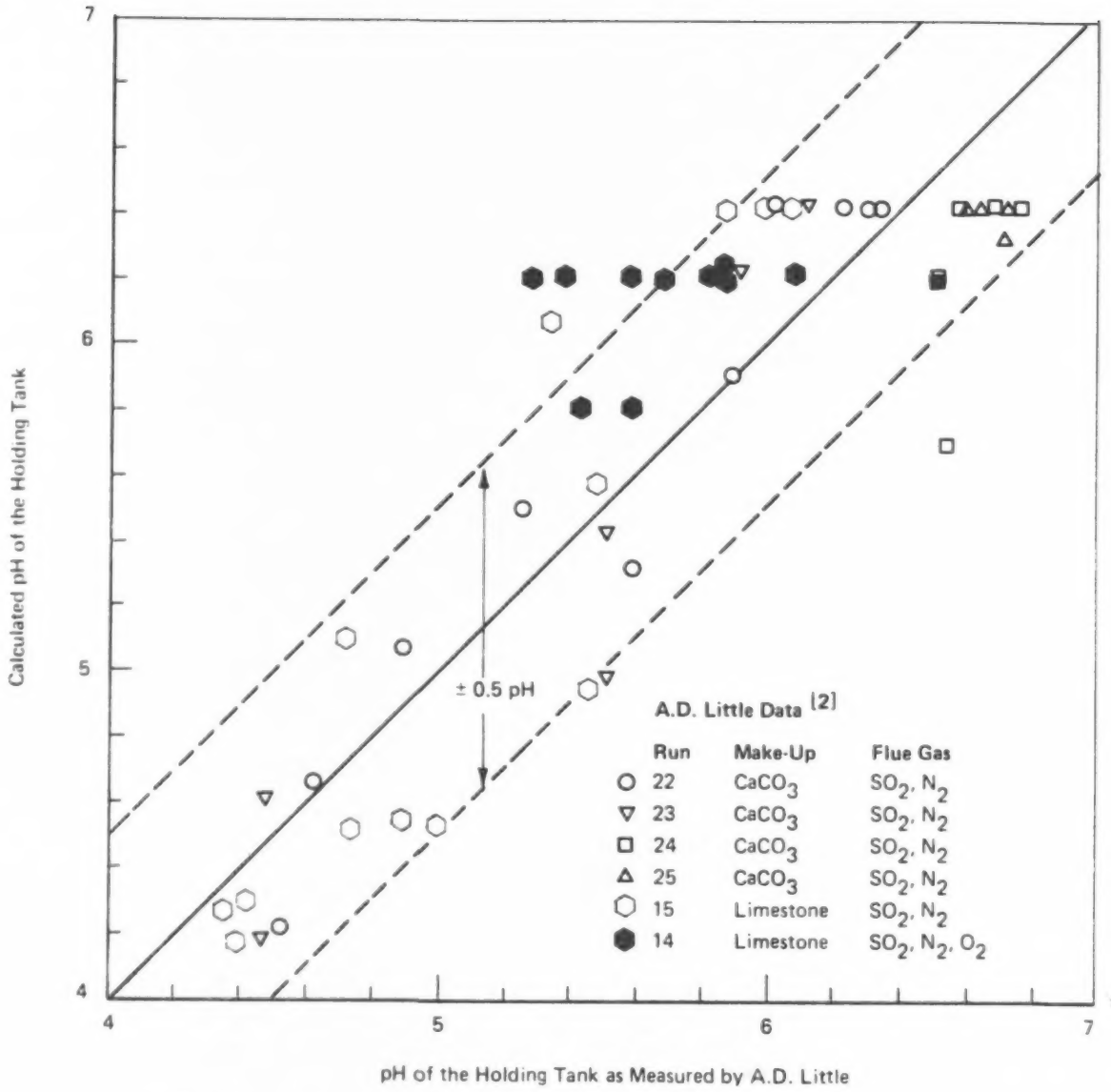

FIGURE VI–7 COMPARISON OF THE CALCULATED AND THE MEASURED HOLDING TANK pH FOR THE A.D. LITTLE SCRUBBER–RECYCLE SYSTEM

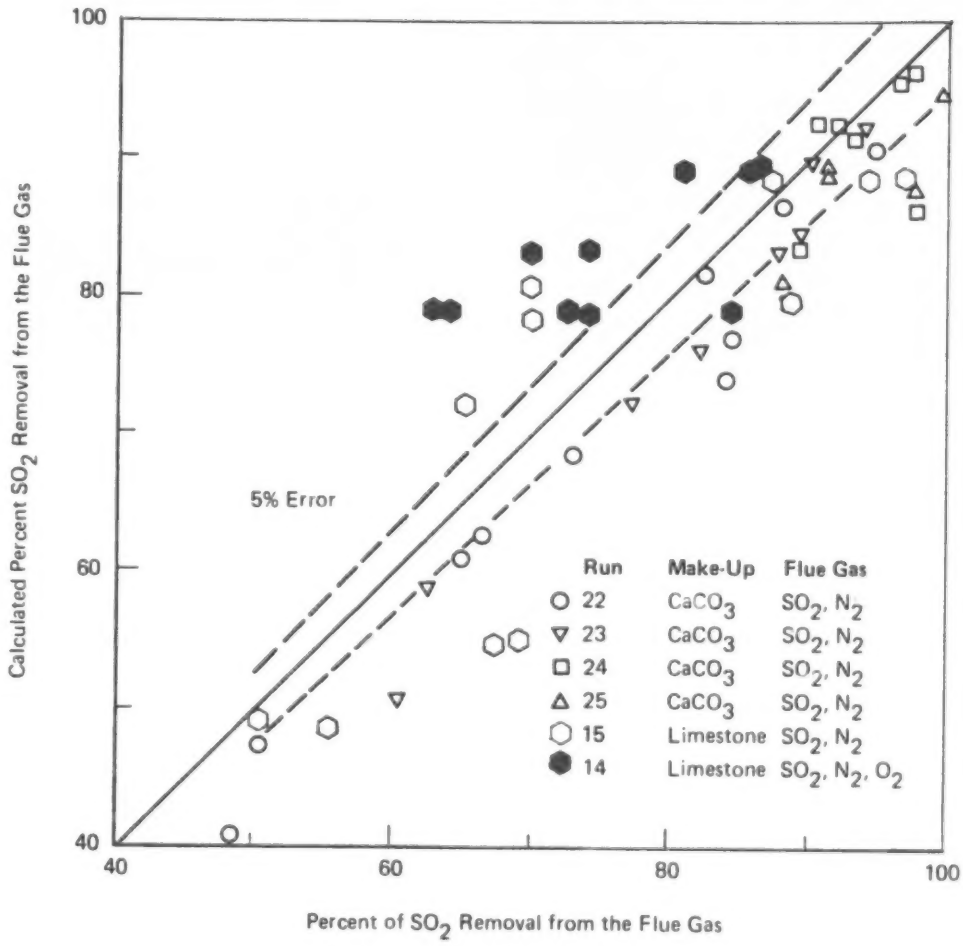

FIGURE VI–8 COMPARISON OF THE CALCULATED AND EXPERIMENTALLY OBSERVED PERCENT SO_2 REMOVAL IN EXPERIMENTAL SCRUBBER–RECYCLE SYSTEM

0.6% $CaCO_3$ with, in one case, the make-up being saturated with respect to $CaSO_4$ and, in the other, no sulfate ions being present. For both these curves it is assumed that none of the sulfur dioxide added to the slurry is oxidized. Also shown in Figure VI-9 is the pH titration curve for 20% oxidation of sulfite to sulfate. For this curve the initial slurry was assumed to contain only $CaCO_3$. By 20% oxidation, it is meant that 20% of the SO_2 goes into the slurry as sulfate ions and the remainder is added as sulfite.

It can be seen from Figure VI-9 that there is little difference between the two oxidation curves and that the 20% oxidation curve lies between them throughout the invariant region. After the invariant region the oxidation curves decrease in pH faster than the no oxidation curves. In general, the rate of decrease in the pH titration curve after the invariant region is greater for larger percent of oxidations. The pH titration curves corresponding to no sulfate-no oxidation and sulfate saturation-no oxidation bound the pH titration curves for the case of $CaCO_3$ make-up with oxidation of sulfite (at least through the invariant region). Hence, these curves can be used to estimate an upper and lower bounds on the pH of the holding tank and the SO_2 removal efficiency in the case of $CaCO_3$ make-up with stoichiometry greater than one. Since these bounds are close to each other, it appears that it is not necessary to know the exact percent oxidation of sulfite to sulfate in order to calculate the pH of the holding tank and SO_2 removal efficiency of the scrubber-recycle system.

After the invariant region the sulfate saturated-no oxygen curve can be used to give an upper found on the pH and SO_2 removal efficiency.

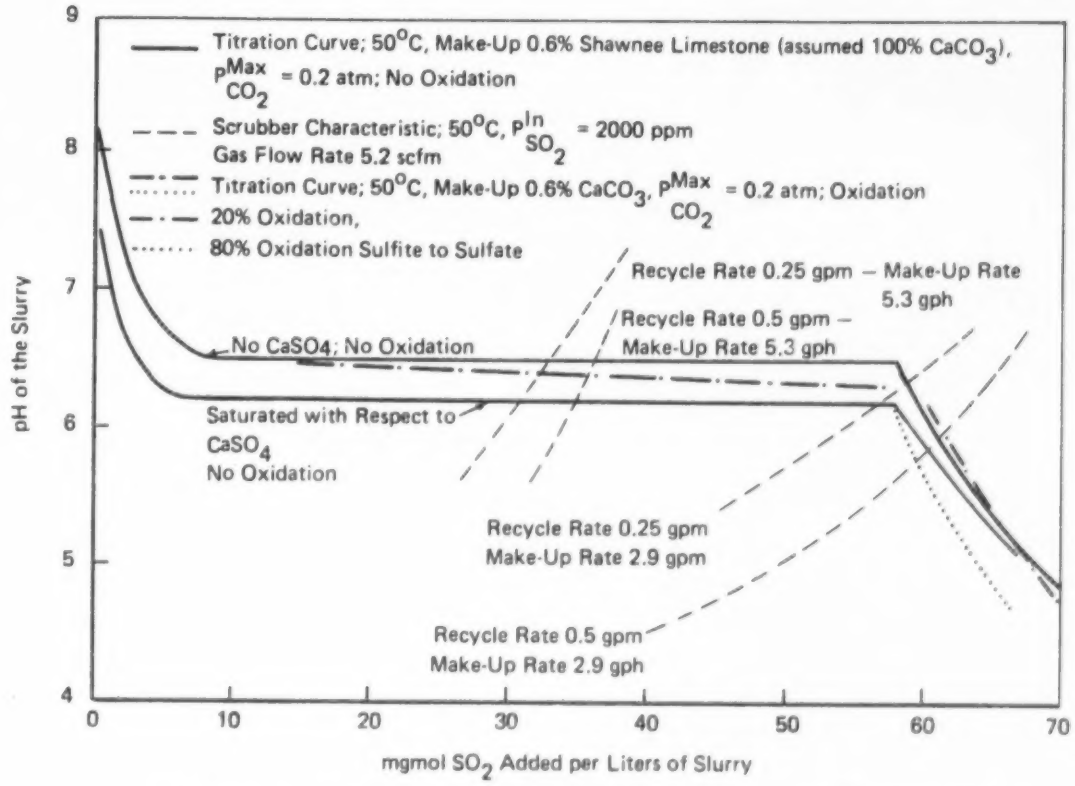
Titration Curve; 50°C, Make-Up 0.6% Shawnee Limestone (assumed 100% $CaCO_3$), $P^{Max}_{CO_2}$ = 0.2 atm; No Oxidation
Scrubber Characteristic; 50°C, $P^{In}_{SO_2}$ = 2000 ppm Gas Flow Rate 5.2 scfm
Titration Curve; 50°C, Make-Up 0.6% $CaCO_3$, $P^{Max}_{CO_2}$ = 0.2 atm; Oxidation
20% Oxidation,
80% Oxidation Sulfite to Sulfate
Recycle Rate 0.25 gpm – Make-Up Rate 5.3 gph
Recycle Rate 0.5 gpm – Make-Up Rate 5.3 gph
No $CaSO_4$; No Oxidation
Saturated with Respect to $CaSO_4$ No Oxidation
Recycle Rate 0.25 gpm Make-Up Rate 2.9 gpm
Recycle Rate 0.5 gpm Make-Up Rate 2.9 gph
pH of the Slurry
9
8
7
6
5
4
0
10
20
30
40
50
60
70
mgmol SO_2 Added per Liters of Slurry

FIGURE VI–9 GRAPHICAL DETERMINATION OF THE OPERATING POINT OF THE SCRUBBER–RECYCLE SYSTEM WITH A COMPARISON OF THE EFFECTS OF EITHER HAVING NO SULFATE OR SULFATE SATURATED SLURRIES

Table VI-3 shows the results of simulating Run 14[2] using the methods described above.

TABLE VI-3

Simulation of Run 14

Inlet SO_2 2000 ppm, Gas Rate 5.2 scfm (4% O_2),
Liquid Temperature 125°F, Make-up 0.6% Shawnee Limestone

Run No.	Observed pH	Calculated pH no $SO_4^=$	Calculated pH sat. $SO_4^=$	Observed % SO_2 Removal	Calculated % SO_2 Removal no $SO_4^=$	Calculated % SO_2 Removal sat. $SO_4^=$
14-1	5.93	6.5	6.2	81	92	89
2	5.45	5.9	5.8	70	83	83
3	5.3	6.35	6.2	64	82	79
4	5.6	6.5	6.2	74	84	79
5	5.9	6.5	6.2	86	92	89
6	5.9	6.5	6.2	85	84	79
7	5.6	5.9	5.8	74	83	83
8	5.4	6.35	6.2	63	82	79
9	5.7	6.5	6.2	73	84	79
10	6.1	6.5	6.2	87	92	89

In this table the pH of the holding tank and SO_2 removal efficiency was calculated using both the no sulfate-no oxygen and saturated sulfate-no oxygen titration curves shown in Figure VI-9. It can be seen from Table VI-3 that the choice of titration curves makes little difference in the calculated pH or SO_2 removal efficiency. However, the titration curve for the saturated sulfate-no oxygen case appears to give better agreement in the calculated and the observed pH's and removal efficiencies.

A comparison between the calculated and observed pH of the holding tank for Run 14 is shown in Figure VI-7 and the comparison of the removal efficiencies is shown in Figure VI-8. While the agreement is not spectacular, it is still good in view of the simplicity of the calculation. It should be noted that the deviation between the observed and calculated SO_2 removal efficiencies is due to the error in predicting the pH of the holding tank. It has already been demonstrated in Figure VI-5 that the scrubber model can predict SO_2 removals with fair precision if the pH of the holding tank is accurately known.

Possible sources of variation between the observed and calculated pH values for Run 14 in Figure VI-7 include:

(1) The assumption that Shawnee limestone is 100% $CaCO_3$. The amount of $CaCO_3$ in the make-up slurry has important consequences in the construction of the titration diagram as discussed previously.

(2) The presence of other elements such as magnesium. The magnesium level in the solution, because of the high solubility of the magnesium salts, will greatly affect the equilibrium compositions which are important in constructing the titration diagram.

REFERENCES

1. Bennett, C. O. and Myers, J. E. Momentum, Heat and Mass Transfer, McGraw-Hill Book Company, Inc., New York, N.Y. (1962).

2. Berkowitz, J. B., Ketteringham, J. M., and Shooter, D. "Evaluation of Problems Related to Scaling in Limestone Wet Scrubbing," report prepared for the EPA (April, 1973).

3. Borgwardt, R. H., EPA Progress Report No. 9 (April, 1973).

4. Leva, M., Tower Packings and Packed Tower Design, The United States Stoneware Company, Akron, Ohio, 2nd Edition (1953).

5. McCabe, W. L. and Smith, J. C. Unit Operations of Chemical Engineering, McGraw-Hill Book Company, Inc., New York, N.Y., 2nd Edition (1967).

6. Treybal, R. E. Mass-Transfer Operations, McGraw-Hill Book Company, Inc., New York, N.Y., 2nd Edition (1968).

7. Vivian, J. E., The Absorption of SO_2 into Lime Slurries: An Investigation of Absorption Rates and Kinetics, report prepared for the HEW Department (September 1973).

8. Wen, C. Y. and Uchida, S. Absorption of SO_2 by Alkaline Solutions in Venturi Scrubber Systems, report prepared for the EPA (July 1973).